https://doi.org/10.5194/egusphere-2026-5535
Preprint. Discussion started: 22 November 2026
© Author(s) 2026. CC BY 4.0 License.

Nonlinear snow–LAP interactions controlling radiative absorption in a tropical Andean glacier

Elver Villalobos-Puma [1,5], Viankcor Cashpa [1,5], Marion Reveillet [2], Christian Torres [3], Thomas Condom [2], Jose-Luis Flores [4], Jose C. Eche-Llenque [5], and Tatiana Boza [1]

[1]Instituto Nacional de Investigación en Glaciares y Ecosistemas de Montaña (INAIGEM), Huaraz, Perú
[2]University Grenoble Alpes, CNRS, IRD, INRAE, Grenoble-INP, Institut des Géosciences de l'Environnement(IGE), Grenoble, France
[3]National Institute for Space Research (INPE),Earth Observation and Geoinformatics Division (DIOTG), Laboratory of Ocean and Atmosphere Studies (LOA), Sao Paulo, Brazil
[4]Instituto Geofísico del Perú (IGP), Lima, Perú
[5]Universidad Nacional Mayor de San Marcos (UNMSM), Facultad de Ciencias Físicas, Lima, Perú

Correspondence: Elver Villalobos-Puma (evillalobos@inaigem.gob.pe)

Abstract. Tropical Andean glaciers are highly sensitive to radiative forcing, yet sub-seasonal spectral albedo variability under shallow and transient snow conditions remains poorly constrained. The coupling between snowpack evolution and light-absorbing particles (LAPs) introduces uncertainties in the representation of surface energy balance. Here, we present the first in situ spectral albedo observations from a tropical Andean glacier, combined with field-based glaciological observations, equivalent black carbon (eBC) measurements, and BioSNICAR radiative transfer simulations. We show that snowpack evolution exerts a strong control on the surface optical response, with snow thinning and progressive exposed ice associated with increasing surface darkening and shortwave absorption. This state-dependent response reflects changes in the surface expression and contribution of LAPs as the glacier evolves during ablation. Simulations constrained by eBC alone are insufficient to reproduce the observed spectral absorption, while the inclusion of mineral dust improves the spectral representation but does not fully account for the observed variability. The additional inclusion of biological impurities provides a more complete representation of the observed spectra, supporting a contribution of biological components to the glacier surface optical response. These results highlight the need to account for surface-state evolution and multiple LAPs in radiative representations of tropical glaciers. The spectral observations provide an observational benchmark for evaluating radiative transfer and surface energy-balance models in tropical Andean glaciers.

1 Introduction

Accelerated glacier mass loss across mountain regions is closely linked to changes in surface energy balance, which is governed by atmospheric conditions regulating radiative fluxes and energy exchange at the glacier-atmosphere interface. In tropical glaciers, where melt is primarily controlled by shortwave radiation and snow cover is shallow and highly transient, surface albedo exerts a first-order control on glacier ablation (Gurgiser et al., 2013; Fyffe et al., 2021). Variations in snowfall, snow persistence, and snowpack evolution regulate the transition from highly reflective snow to darker glacier ice, producing a

https://doi.org/10.5194/egusphere-2026-5535
Preprint. Discussion started: 22 November 2026
© Author(s) 2026. CC BY 4.0 License.

strong snow-to-ice albedo feedback. These transitions can occur over short timescales in response to changes in atmospheric conditions and intra-seasonal precipitation variability, making surface albedo particularly sensitive to transient snow conditions. In the tropical Andes, regional differences in glacier response have been associated with differences in temperature and precipitation, highlighting the importance of climatic conditions in regulating glacier retreat (Li et al., 2019).

The LAPs, particularly black carbon (BC) associated with anthropogenic emissions and biomass burning, are important contributors to snow darkening. The BC is considered the most efficient light-absorbing particle per unit mass, reducing snow and ice albedo, enhancing radiative absorption, and modifying the optical properties of the snowpack, thereby accelerating glacier melt (Bond et al., 2013; Shi et al., 2020; Fierce et al., 2016; Niu et al., 2020; Gatti et al., 2023; Meng et al., 2025). Other LAPs, including mineral dust and biological impurities, can also contribute to snow darkening, depending on their abundance and optical properties (Kang et al., 2020; Chen et al., 2024; Reynolds et al., 2025). Their radiative impact depends not only on particle composition and concentration but also on snowpack evolution, which controls impurity exposure and surface enrichment during ablation. However, observational constraints in tropical Andean glaciers remain limited. In particular, in situ spectral albedo measurements remain scarce, and existing studies have focused primarily on BC, with limited evaluation of the combined influence of different LAPs and snowpack evolution on spectral albedo and radiative forcing. Despite these advances, how snowpack evolution interacts with different LAPs to control radiative absorption in tropical Andean glaciers remains poorly understood.

Spectral albedo, defined as the wavelength-dependent reflectance of snow and ice, provides detailed information on the influence of physical and microphysical properties, as well as the presence of LAPs such as BC and biological impurities (snow and ice algae). In contrast, broadband albedo represents the integrated reflectance over a wide spectral range and has been more widely measured in Andean glaciers (Gurgiser et al., 2013; Sicart et al., 2014; Condom et al., 2018), whereas observational studies of spectral albedo across tropical Andean glaciers remain limited. While studies in other regions have quantified the impact of multiple LAPs, including BC and biological impurities (Cook et al., 2017; Chevrollier et al., 2025), research in the Andes has primarily focused on BC (e.g., Schmitt et al., 2015; Torres et al., 2018; Soto Carrión et al., 2021; Bonilla et al., 2023). Although these efforts have been fundamental for understanding its role, the lack of spectral albedo observations limits a comprehensive assessment of different albedo-forcing agents in Andean glaciers. In particular, the contribution of different LAPs, including biological impurities and mineral dust, to spectral albedo variability in tropical Andean glaciers remains poorly quantified, hindering a process-based understanding of glacier surface reflectance.

The radiative impact of LAPs, including BC, mineral dust, and biological impurities, depends not only on their composition and concentration but also on the physical evolution of the snowpack. In tropical glacier environments, characterized by persistently high solar radiation and shallow, transient snow cover, surface albedo is highly dynamic and sensitive to short-term snow accumulation and ablation processes. As snow thins during ablation, LAPs become progressively concentrated near the surface, enhancing shortwave absorption and accelerating melt. This response is inherently nonlinear, since small reductions in snow thickness can trigger disproportionate increases in radiative absorption, particularly during the transition from snow-covered to exposed-ice surfaces (Doherty et al., 2013; Flanner et al., 2021; Fyffe et al., 2025). The evolving snowpack becomes a key

https://doi.org/10.5194/egusphere-2026-5535
Preprint. Discussion started: 22 November 2026
© Author(s) 2026. CC BY 4.0 License.

factor controlling the magnitude of LAP-induced radiative forcing, highlighting the importance of considering transient snow conditions when assessing glacier surface energy balance.

Regionally, quantifying the effects of LAPs on the tropical Andean cryosphere still presents significant limitations, despite recent advances in understanding their contribution to glacier retreat (Soto Carrión et al., 2021; Gilardoni et al., 2022; Bonilla et al., 2023; Ontiveros-Gonzalez et al., 2025). In the tropical Andes, BC deposition has been shown to generate persistent positive radiative forcing even at low concentrations (Bonilla et al., 2023), while studies from other mountain regions indicate that interactions among multiple LAPs can substantially amplify snow darkening and melt processes (Kang et al., 2020; Chen et al., 2024). These limitations are further associated with local conditions, including the short duration of snow cover, cloudiness modulated by Amazonian influence, surface roughness, and the high spatial and temporal heterogeneity of atmospheric particles (Villalobos-Puma et al., 2024b; Chevrollier et al., 2025). These factors also make the detection and quantification of optical changes over small glacier surfaces using remote sensing particularly challenging, especially for BC. Furthermore, the scarcity of sustained in situ observations limits the characterization of seasonal variability in LAPs deposition, increasing uncertainty in estimates of surface albedo and radiative forcing. These limitations highlight the need to improve understanding of LAPs-radiation interactions in tropical glacier environments.

To address these regional limitations, the Huaytapallana Cordillera was selected as the study site due to its representativeness of tropical Andean glaciers and its logistical accessibility for conducting high-frequency in situ campaigns, as well as its proximity to urban centers, biomass burning areas, and the influence of the Amazon Basin as relevant sources of absorbing aerosols, including BC (Villalobos-Puma et al., 2024b). These conditions, combined with high levels of solar radiation during the dry season and intra-seasonal dry periods, increase the susceptibility of the glacier surface to LAP-induced albedo feedback, promoting albedo reduction and enhanced ablation, with direct implications for regional water availability. Additionally, local valley-mountain circulation patterns facilitate the transport of aerosols from emission regions to glacier surfaces, reinforcing deposition processes. To characterize these processes, the integration of in situ observations with radiative transfer simulations provides a robust framework for quantifying the temporal variability of LAPs deposition and its radiative impact on the tropical cryosphere (Skiles et al., 2018). The unique combination of continuous atmospheric BC measurements, snow BC observations, and in situ spectral albedo measurements provides strong observational constraints for radiative transfer simulations, enabling a more robust interpretation of the potential contribution of different LAPs to glacier surface albedo and radiative forcing.

Building upon this observational framework, this study combines high-resolution in situ spectral albedo observations with radiative transfer modeling to investigate how snowpack evolution and light-absorbing particles (LAPs) shape the spectral radiative response of a tropical Andean glacier. Specifically, we (1) characterize atmospheric and snow BC and present, to our knowledge, the first in situ spectral albedo observations from Yanaucsha Glacier in the Huaytapallana Cordillera, central Peruvian Andes; and (2) use the BioSNICAR radiative transfer model to assess how variations in snow physical and microphysical properties and LAPs, including BC, mineral dust, and biological impurities, can explain the observed spectral albedo. By constraining the model with in situ spectral observations, we explore the relative contribution of snowpack properties and different impurity types to the observed radiative response under evolving tropical snow conditions. This integrated observa-

https://doi.org/10.5194/egusphere-2026-5535
Preprint. Discussion started: 22 November 2026
© Author(s) 2026. CC BY 4.0 License.

tional–modeling framework provides a process-based perspective on the controls of spectral albedo and LAP-induced radiative effects, with implications for understanding surface energy absorption and ablation in tropical Andean glaciers.

2 Study area and observational data

The Yanaucsha Glacier, located in the Huaytapallana mountain range in the Central Andes of Peru (11.938°S, 75.069°W) at 5000 m a.s.l., is situated within the outer humid tropical domain. Its atmospheric regime is influenced by moisture transport from the Amazon basin and Pacific-origin flows, while orographic forcing and mountain-valley circulation coupled with radiative cooling promote solid precipitation at high elevations (Villalobos-Puma et al., 2024a). Disdrometer observations show that solid and liquid precipitation contribute similarly on a daily basis (49% and 51%, respectively), although snowfall dominates at night (78%), playing a key role in glacier accumulation processes (Llactayo et al., 2024).

The Yanaucsha Glacier presents distinct accumulation and ablation zones (Fig. 1b), making it an ideal site for assessing LAPs deposition and glacier surface evolution. Deep valleys connecting the Amazon basin with high-elevation regions enhance the transport of absorbing aerosols toward the glacier surface (Villalobos-Puma et al., 2024b), increasing its sensitivity to radiative forcing by LAPs. To investigate these processes, two complementary monitoring sites were established: (i) the Mountain Glacier and Ecosystem Monitoring Center (CEMGEM) of INAIGEM, located near the glacier front at 4710 m a.s.l. (Figs. 1b,e), and (ii) a glacier-surface site for spectral albedo and deposited BC measurements in snow and ice (Figs. 1c,d). These observations enable characterization of atmospheric and deposited eBC variability in a high-mountain tropical glacier environment.

2.1 Field observations and monitoring strategy

2.1.1 Continuous atmospheric and glaciological measurements

Atmospheric and glaciological observations were conducted in the study region between 2022 and 2026. Continuous atmospheric measurements at the CEMGEM included eBC concentrations from an AE33 Aethalometer and precipitation phase from a Parsivel disdrometer. These datasets have been previously used to characterize atmospheric BC variability, transport dynamics, and precipitation phase in the central Peruvian Andes (Villalobos-Puma et al., 2024a; Llactayo et al., 2024), and are here used to evaluate atmosphere–glacier interactions associated with BC deposition.

Monthly in situ glaciological observations were conducted primarily within the glacier ablation zone. Field observations included sky conditions (clear or overcast), which were used to classify incoming solar radiation as predominantly direct or diffuse, sampling time for solar zenith angle (SZA) estimation, snow depth and density, and surface snow sampling over 50 cm × 50 cm areas for deposited eBC quantification. The SZA was estimated using local time, geographic coordinates, and the elevation of the sampling points. Observations covered both wet-season conditions associated with fresh snow cover and dry-season conditions characterized by firn, discontinuous snow cover, and exposed ice surfaces. During periods of intense melting,

https://doi.org/10.5194/egusphere-2026-5535
Preprint. Discussion started: 22 November 2026
© Author(s) 2026. CC BY 4.0 License.

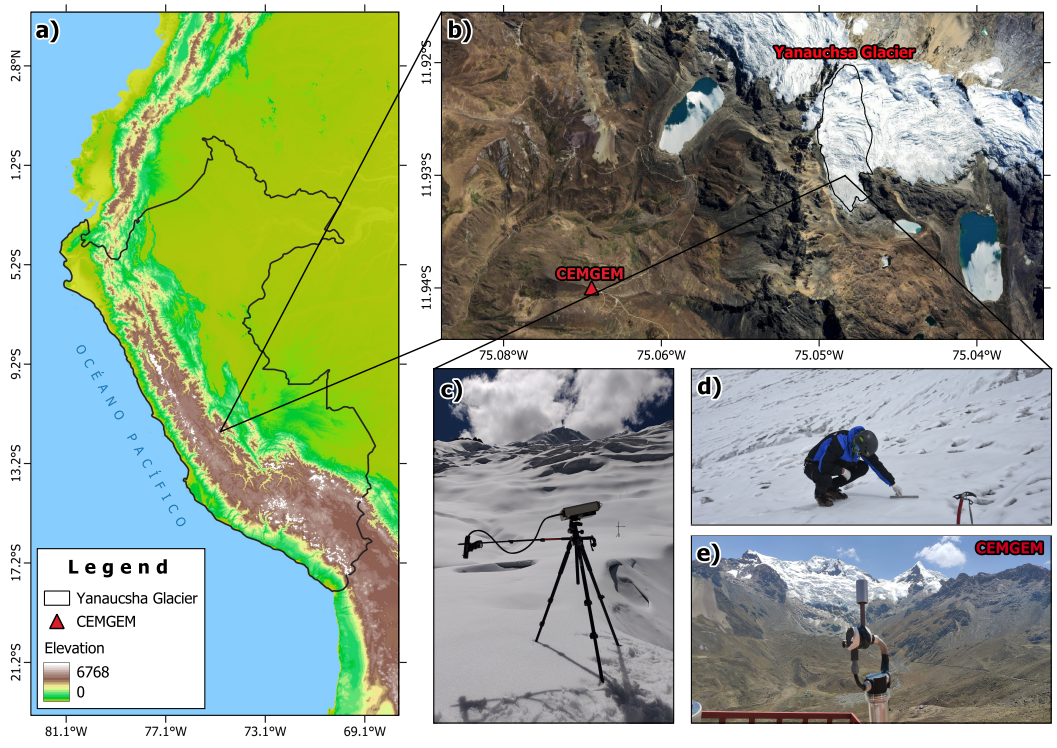


Figure 1. Study area and monitoring activities conducted during the 2022-2026 period. a) Location of the Huaytapallana Cordillera in the Central Andes of Perú. b) Southern sector of the Huaytapallana Cordillera, showing the Yanaucsha Glacier outlined in black and the Mountain Glacier and Ecosystem Monitoring Center (CEMGEM) marked in red at 4710 m of elevation, c) Spectroradiometer installed on the glacier surface for spectral reflectance measurements. d) Continuous in situ glaciological measurements on the Yanaucsha Glacier. e) Continuous atmospheric BC measurements at CEMGEM.

sampling activities were shifted toward the accumulation zone to preserve the temporal continuity of the observations. Snow density was estimated using the volumetric method ($\rho = \frac{m}{V}$), while snow depth was derived from multiple-point measurements.

Surface albedo was continuously monitored using a low-cost albedometer following Condom et al. (2018), with measurements recorded every 5 min. A daily albedo index was defined as the mean albedo between 11:00 and 14:00 LT to minimize SZA effects. These broadband albedo observations were used to characterize glacier surface conditions across seasonal and intra-seasonal timescales and to support the interpretation of the spectral albedo observations. Deposited eBC concentrations on the glacier surface were determined using the Light Absorption Heating Method (LAHM) (Schmitt et al., 2015, 2022). Surface snow samples were melted, filtered through quartz fiber filters, and analyzed by measuring the thermal response induced by visible-radiation absorption by light-absorbing particles. The resulting signal was converted into eBC concentrations expressed as nanograms per gram of snow ($\mathrm{ng\,g^{-1}}$).

https://doi.org/10.5194/egusphere-2026-5535
Preprint. Discussion started: 22 November 2026
© Author(s) 2026. CC BY 4.0 License.

2.1.2 Spectral albedo survey campaigns

Spectral albedo measurements were performed using a calibrated HR-1024i spectroradiometer (Spectra Vista Corporation, SVC), with spectral resolution ranging from 1.5 to 6 nm over the 340–2500 nm range. The instrument measured reflected radiance from the glacier surface and incident solar irradiance using interchangeable downward- and upward-facing optical configurations. Measurements followed standard field spectroradiometric protocols, with the optical fiber positioned 60 cm above the surface.

Two campaigns were conducted under contrasting snow conditions. The first, on 3 June 2025, was performed under continuous snow cover (mean snow thickness: 9.6 cm) at seven sites across the glacier front. Ten spectra were acquired at each site, covering surfaces from clean snow to visibly impurity-rich snow. The second campaign, conducted on 27 August 2025, targeted discontinuous snow cover and exposed ice conditions along an altitudinal gradient between 4900 and 5000 m a.s.l. Measurements in both campaigns were carried out between 11:00 and 13:00 LT under clear-sky conditions to minimize high solar zenith angle effects. Radiometric calibration using a certified reference panel was performed before and after each survey. The measured spectral irradiance and reflectance constitute the observational dataset used in the BioSNICAR simulations described in Sect. 2.2

2.2 Methodology

2.2.1 Data processing and surface classification

Atmospheric eBC concentrations measured by the AE33 aethalometer at 1 min resolution were aggregated into hourly, daily, and monthly averages to construct climatological and temporal datasets representative of high-elevation conditions at CEMGEM. Glaciological observations, including snow depth, snow density, broadband albedo, and deposited eBC concentrations, were compiled from monthly field campaigns to characterize the seasonal evolution of snowpack properties. To minimize the influence of local meltwater redistribution, the deposited eBC climatology was derived from the upper sampling site, providing a more representative estimate of atmospheric deposition. These processed datasets were used to construct the climatological and temporal analyses of atmospheric eBC, deposited eBC, snow properties, and broadband albedo.

Measured spectral albedo observations were resampled to a uniform spectral resolution of 10 nm to facilitate comparison among field campaigns and subsequent model simulations. According to snow cover conditions, the spectra were classified into three surface types: continuous snow (CS), characterized by a mean snow thickness of approximately 12 cm over glacier ice; thin snow (TS), corresponding to discontinuous snow cover with an average thickness of about 2 cm; and exposed ice surface (IE), characterized by glacier ice or firn covered by a residual snow layer averaging approximately 0.5 cm. The effective snow grain radius (r_{eff}), representing the snow microstructure, was estimated through spectral sensitivity analysis by minimizing discrepancies between observed and simulated spectra in the 0.8-2.5 μm range. This wavelength interval is dominated by ice absorption, whereas the influence of LAPs is minimal (Chevrollier et al., 2023), providing a robust and physically consistent estimate of the effective snow grain radius. The processed spectral observations, surface classification, and derived snow microphysical properties constitute the observational basis for the BioSNICAR simulations.

https://doi.org/10.5194/egusphere-2026-5535
Preprint. Discussion started: 22 November 2026
© Author(s) 2026. CC BY 4.0 License.

2.2.2 BioSNICAR model configuration

The spectral albedo of snow and ice on the glacier surface was simulated using the one-dimensional radiative transfer model BioSNICAR (Snow, Ice, and Aerosol Radiative model with a bio-optical module) (Cook et al., 2020), an extension of the SNICAR model (Flanner et al., 2007). This model solves the radiative transfer equation under the plane-parallel assumption, allowing the estimation of spectral reflectance and transmittance of stratified snow and ice layers. The anisotropic scattering of snow and ice particles is described through a multiple scattering parameterization based on Mie theory, numerically solved using the adding-doubling approach (Whicker et al., 2022). This formulation captures the interaction of solar radiation with snow and ice considering key physical parameters such as density, thickness, effective grain size, and the concentration of LAPs. On this physical basis, BioSNICAR incorporates a bio-optical module that parameterizes the contribution of biological impurities. The parameterization proposed by Cook et al. (2017) (hereafter, COOK) represents the optical properties of snow and glacier algae derived from their pigment composition within the radiative transfer scheme. The parameterization proposed by Chevrollier et al. (2023) (hereafter, CHEV) represents biological impurities using experimentally derived optical properties of pigmented snow and ice microalgae. Mineral dust (MD) was also included as an additional LAPs using its corresponding optical parameterization (Cook et al., 2020; Di Mauro et al., 2024).

The model has been widely used to investigate the radiative effects of LAPs on snow and ice albedo. In this study, the simulations were strongly constrained by field observations, with the glacier surface properties and eBC concentrations prescribed from the in situ measurements described in Sect. 2.2.1. Radiative conditions were defined according to the type of incident radiation (diffuse or direct) and the solar zenith angle, calculated based on the latitude, longitude, and altitude of the sampling sites. To avoid the influence of orographic shading, a maximum solar zenith angle of 82° was set. Additionally, a spectral irradiance profile representative of high-mountain conditions was used to prescribe the spectral distribution of incoming solar radiation at the glacier surface.

To evaluate the contribution of LAPs other than eBC to glacier spectral albedo, a baseline Physical-Optical (PO) configuration was established using the observed physical and optical properties and measured eBC concentrations for each sample. This configuration represents the reference surface state without additional LAPs. Starting from the PO configuration, mineral dust was incorporated to evaluate its ability to explain the remaining discrepancies between simulated and observed spectral albedo. Subsequently, the combined contribution of mineral dust and biological impurities was evaluated using the COOK and CHEV parameterizations, considering snow algae and ice algae. In these simulations, the observed physical properties and eBC concentration were kept fixed, while the concentrations of the additional LAPs were adjusted to evaluate their contribution to the spectral fit.

The vertical representation of the snowpack was defined according to snow thickness. For thicknesses greater than 2 cm, a three-layer configuration was adopted following the methodology of Cook et al. (2017): a 3 mm surface layer, a 2 cm eBC-contaminated middle layer, and a third layer corresponding to the remaining snow thickness. For snow thicknesses ≤ 2 cm, a two-layer configuration was used: a 3 mm surface layer and a second layer corresponding to the remaining thickness,

https://doi.org/10.5194/egusphere-2026-5535
Preprint. Discussion started: 22 November 2026
© Author(s) 2026. CC BY 4.0 License.

contaminated with eBC. Due to the higher uncertainty associated with discontinuous snow thicknesses, a ± 1 cm error margin was considered in this case.

2.2.3 Radiative forcing and snowmelt induced by BC

Radiative forcing and the associated eBC-induced melt were calculated following the approach of Chevrollier et al. (2023, 2025). The broadband albedo (BBA) was computed as

$$BBA = \frac{\sum \alpha(\lambda)\, IR(\lambda)}{\sum IR(\lambda)} \tag{1}$$

where λ is the wavelength (μm), $\alpha(\lambda)$ is the spectral albedo, and $IR(\lambda)$ is the incident spectral irradiance (measured in the field or, when unavailable, using the spectrum implemented in BioSNICAR). The spectral range considered (0.35–2.5 μm) corresponds to the shortwave domain relevant to the glacier surface energy balance.

The radiative forcing induced by eBC at the glacier surface was calculated as

$$RF_{eBC} = IR\,(BBA_{without} - BBA_{with}) \tag{2}$$

where IR is the incident shortwave irradiance (W m^{-2}).

Hourly radiative forcing was calculated between 08:00 and 17:00 local time (LT) using the corresponding incoming shortwave irradiance. Incoming shortwave irradiance was measured at CEMGEM during $2023-2026$, whereas missing observations in 2022 were complemented using ERA5 reanalysis.

The potential $eBC-induced$ melt equivalent was estimated by assuming that all additional absorbed energy was available for ice melt. Using the latent heat of fusion of ice ($L_f = 334000$ J kg^{-1}), the daily melt mass was calculated as

$$M_m = \frac{\sum RF_h \cdot 3600}{L_f} \tag{3}$$

where RF_h is the hourly radiative forcing (W m^{-2}), 3600 is the number of seconds per hour, and M_m is the daily eBC-induced melt mass (kg m^{-2} d^{-1}). Melt was expressed as centimetres of water equivalent (cm w.e. d^{-1}), assuming that 1 kg m^{-2} is equivalent to 1 mm water equivalent; thus, values were divided by 10 to convert millimetres to centimetres.

3 Results

3.1 Seasonal variability of glacier surface properties

Monthly climatologies of atmospheric eBC concentrations measured at CEMGEM and eBC deposited in snow with the evolution of snow depth and snow density in the glacier ablation zone, reveal their seasonal variability during the 2022-2026 period

https://doi.org/10.5194/egusphere-2026-5535
Preprint. Discussion started: 22 November 2026
© Author(s) 2026. CC BY 4.0 License.

(Fig. 2). These variables allow the analysis of the deposition and accumulation dynamics of eBC in relation to the physical state of the glacier surface and snowpack conditions. Atmospheric eBC (Fig. 2a) exhibits a well-defined unimodal seasonal pattern, with a pronounced maximum in September and a high dispersion toward extreme values. The most frequent concentrations occur during the dry season and the transition period toward the wet season (July-November), indicating a marked seasonal enhancement of atmospheric BC loading under reduced wet removal conditions. Consistently, the estimated concentrations on the glacier surface (Fig. 2b) also increases between July and November, in agreement with the atmospheric maximum, indicating a coherent seasonal coupling between atmospheric availability and surface deposition. However, particularly high values recorded in March reveal a partial decoupling from the atmospheric pattern, suggesting that surface eBC variability is not solely controlled by instantaneous atmospheric concentrations but also by surface processes operating within the snowpack. During periods of intense ablation, the progressive reduction of snow depth and the exposure of underlying glacier ice favor the surface enrichment of previously deposited LAPs. An inverse relationship is observed between snow depth and eBC concentration, suggesting a volumetric concentration effect associated with snowpack thinning. This process likely enhances shortwave radiative forcing through the LAP-induced albedo feedback mechanism. This behavior is especially evident in 2024, when extreme outlier values were observed in glacier snow (Fig. 2b), coinciding with the 2023-2024 El Niño event and a period characterized by intense biomass-burning episodes at lower elevations and regional intrusions of carbonaceous aerosols into the glacier environment.

These results suggest that the surface state of the glacier exerts a first-order control on impurity concentration through physical redistribution and re-exposure processes. Regarding snow depth (Fig. 2c), a well-defined annual cycle is observed, with maxima exceeding 50 cm between February and May during the wet season. This pattern is accompanied by marked intermonthly variability, particularly toward lower values associated with reduced snow cover. In contrast, during July-October, corresponding to the dry season in the ablation zone, snow depth tends toward near-zero values, reflecting ablation-dominated conditions and prolonged exposure of the glacier surface to direct radiative forcing. Snow density (Fig. 2d) exhibits a clear seasonal cycle, with higher values during the wet season and lower values during the dry season. This pattern reflects the influence of hydroclimatic conditions on snowpack properties, with higher densities associated with enhanced snow metamorphism under near-melting conditions, and lower densities corresponding to reduced accumulation and dry period.

Although the seasonal climatology presented above captures the general co-variability between atmospheric eBC, snow conditions, and surface impurities, it does not resolve the short-term transitions associated with precipitation intermittency and episodic atmospheric loading. To address this limitation, Figure 3 examines the temporal evolution of these processes at intraseasonal scales. Under background conditions, atmospheric eBC concentrations remain around 0.4 μg m^{-3}; however, abrupt increases are observed during periods of enhanced atmospheric loading (Fig. 3c). From 16 August onward, episodes with concentrations close to 1.2 μg m^{-3} are identified, coinciding with elevated atmospheric eBC levels associated with regional biomass-burning emissions. Peak concentrations reach approximately 1.8 μg m^{-3}, followed by marked decreases, such as those observed on 25 August and on 6 and 17 September 2024. These declines coincide with precipitation events, suggesting efficient BC removal through wet deposition. The temporal synchrony between concentration decreases and the occurrence of solid precipitation indicates that snowfall plays an important role in transferring BC from the atmosphere to the glacier surface.

https://doi.org/10.5194/egusphere-2026-5535
Preprint. Discussion started: 22 November 2026
© Author(s) 2026. CC BY 4.0 License.

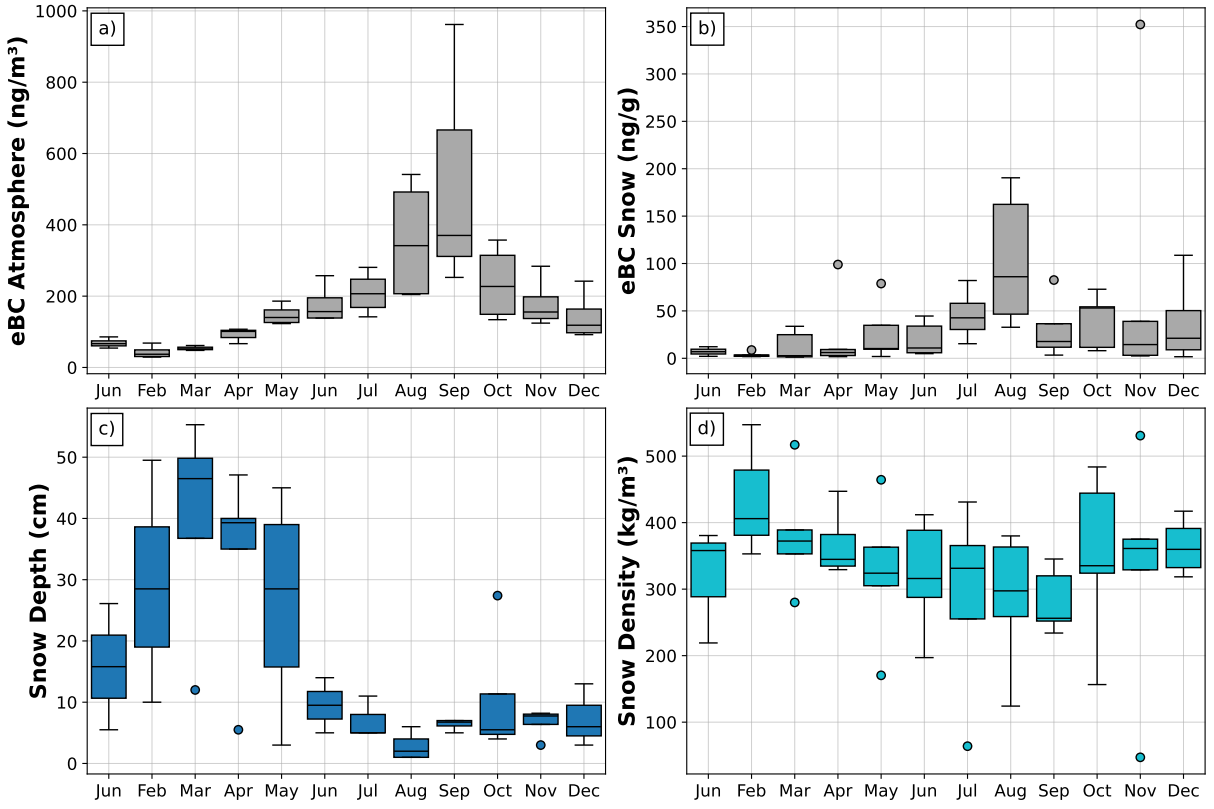


Figure 2. Monthly climatology of glaciological and atmospheric parameters for the 2022-2026 period, a) atmospheric eBC concentration (ng/m^3), b) eBC in glacier snow (ng/g), c) snow depth (cm) and (d) snow density (kg/m^3). Boxplots represent the median, interquartile range, and outliers (circles).

Surface albedo exhibits pronounced seasonal and intraseasonal variability (Fig. 3a) between May 2025 and April 2026 and closely follows variations in snow depth (Fig. 3b), highlighting the strong dependence of surface reflectivity on snow-cover persistence. Snowfall events produce simultaneous increases in snow depth and albedo through surface renewal, whereas prolonged periods without solid precipitation promote snow depletion and a rapid decline in albedo associated with the progressive exposure of glacier ice. A notable feature is that snow loss does not occur simultaneously across the glacier. During the dry season, snow depletion progresses from lower to higher elevations, revealing an altitudinal snow-persistence gradient. The ablation zone exhibits the fastest response, with abrupt decreases in both snow depth and albedo following the cessation of snowfall, whereas higher elevations maintain snow cover and highly reflective conditions for considerably longer periods. This behavior indicates that snow persistence exerts a first-order spatial control on glacier albedo, generating pronounced heterogeneity in the glacier's radiative conditions. The early exposure of glacier ice at lower elevations promotes a premature reduction in surface reflectivity and an increase in absorbed shortwave radiation, whereas persistent snow cover at higher elevations delays this transition.

https://doi.org/10.5194/egusphere-2026-5535
Preprint. Discussion started: 22 November 2026
© Author(s) 2026. CC BY 4.0 License.

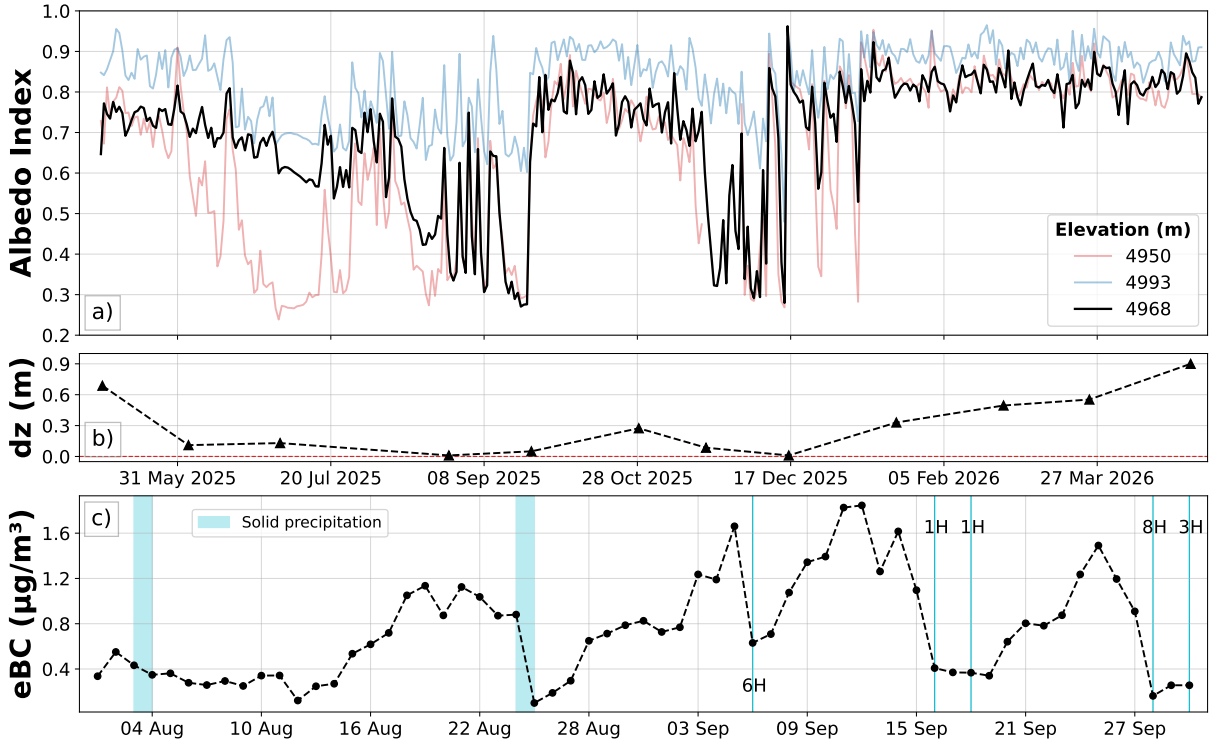


Figure 3. Surface albedo measured on the glacier during (a) the dry and wet seasons, (b) snow depth (dz) measurements, and (c) the time series of eBC measured outside the glacier at 4710 m a.s.l. Light-blue shaded bars indicate solid precipitation events. The values shown in hours (H) correspond to the duration of each precipitation event.

Furthermore, Figure 3a shows that the wet season does not necessarily constitute a radiatively stable state. Periods of several consecutive days without snowfall promote rapid snow-cover depletion in the ablation zone, reflected by decreases in snow depth and abrupt reductions in albedo to values comparable to those observed during the dry season. These episodes drive rapid transitions from snow-covered to exposed ice surfaces and reveal pronounced intraseasonal variability in the glacier's radiative response. Rather than being characterized by progressive snow depletion, the wet season is dominated by recurrent cycles of snow accumulation and disappearance associated with snowfall intermittency. The results demonstrate a high sensitivity of glacier surface conditions to relatively short interruptions in solid precipitation, even during the period of maximum precipitation. The results show that snow-cover persistence constitutes the primary link between precipitation variability and the glacier's radiative response. The close correspondence between snow depth and albedo indicates that the evolution of surface conditions depends not only on the occurrence of snowfall events, but also on the duration of snow cover over the glacier surface.

https://doi.org/10.5194/egusphere-2026-5535
Preprint. Discussion started: 22 November 2026
© Author(s) 2026. CC BY 4.0 License.

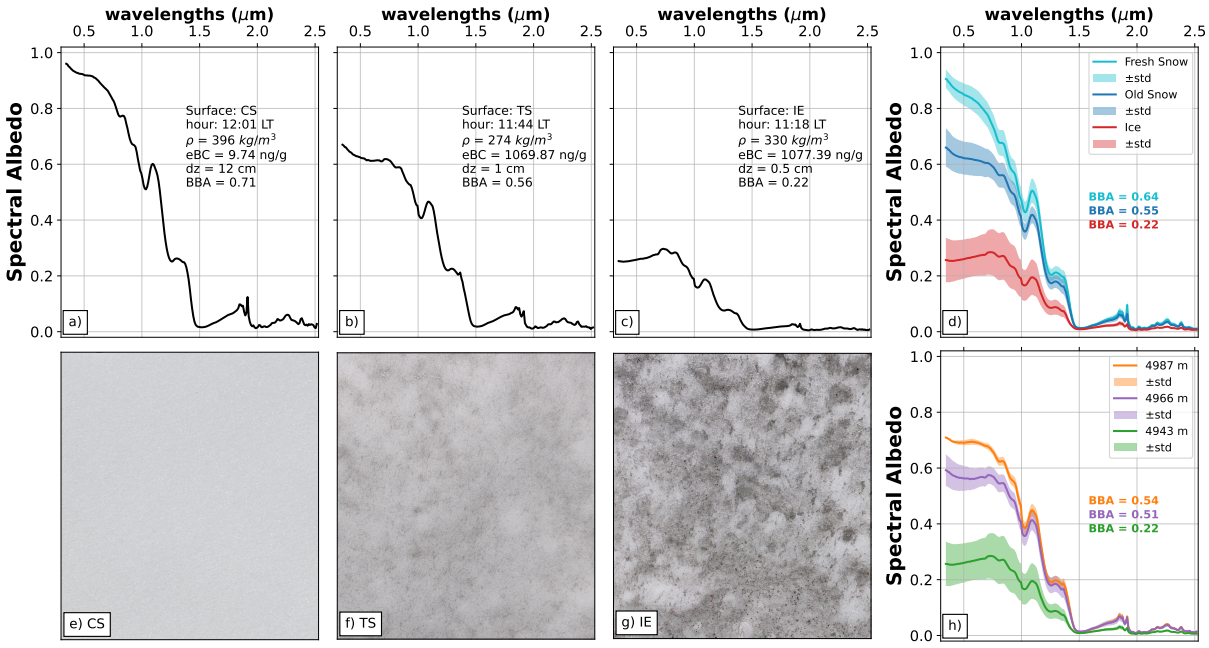


Figure 4. Spectral albedo observed during the measurement campaigns on Yanaucsha Glacier. a) and e) CS state, b) and f) TS state, c) and g) IE state, d) grouped spectral according to surface type (CS, TS, IE), and h) spectral variation with altitude.

3.2 Glacier surface spectral albedo: observations and BioSNICAR modeling

Figure 4 shows the spectral albedo measured on the glacier surface for three surface states defined by snowpack thickness: continuous snow (CS; 12 cm), thin snow (TS; 2 cm), and ice-exposed surfaces (IE; 0.5 cm). The CS state exhibits the highest spectral albedo values (Fig. 4a), exceeding 0.9 in the visible range, consistent with high reflectance conditions. In contrast, the TS state shows a marked decrease in spectral albedo, particularly in the visible and near-infrared regions (Fig. 4b), associated with increased impurity concentration and reduced snow thickness.

The TS state shows a marked decrease in spectral albedo, particularly in the visible range and partially in the near-infrared (Fig. 4b). This behavior coincides with a substantial increase in eBC concentration (1069.87 ng/g) and a reduction of the BBA to 0.56. The IE state (Fig. 4c) exhibits the lowest spectral albedo, with a BBA of 0.22, consistent with a surface dominated by glacier ice and the intrinsic absorption of the underlying material. The transition from CS to TS and IE therefore reflects not only decreasing snow thickness, but also an increasing optical influence of the underlying glacier ice as the snow layer becomes thinner. Furthermore, as the snow layer decreases, the glacier surface darkens, a pattern typical of the ablation zone. The results show a strong sensitivity of spectral albedo to changes in snowpack thickness, with a progressive decrease from snow-covered y el cambio de la tasa de envejecimiento de la nieve to exposed ice conditions. This pattern is associated with snow aging and the effective increase in grain size, which influence the interaction between solar radiation and the glacier surface.

https://doi.org/10.5194/egusphere-2026-5535
Preprint. Discussion started: 22 November 2026
© Author(s) 2026. CC BY 4.0 License.

In the visible and near-ultraviolet range, pronounced spectral contrasts are observed between CS and IE surfaces. In CS, albedo progressively increases toward shorter wavelengths, whereas in IE the opposite occurs, with a decrease reflecting the dominant absorption by exposed ice. This pattern is consistent with the average spectra grouped for the three surface states (Fig. 4d). Spectral separation between the states intensifies below 1.5 μm, from the near-infrared toward the near-ultraviolet. As snow ages and snowpack thickness decreases, albedo declines across the near-ultraviolet, visible, and near-infrared ranges, implying an increase in energy absorption by the glacier surface. This effect is particularly significant in the near-infrared, where the lower albedo increases shortwave absorption by the glacier surface.

The spectra exhibit a clear altitudinal variation along the transect from the ablation zone to the accumulation zone (Fig. 4h). In the lower zone, exposed ice surfaces with low albedo dominate, whereas at higher elevations thin layers of crystalline snow gradually increase albedo, although they do not reach values typical of fresh snow. This altitudinal gradient highlights the influence of surface conditions on the modulation of glacier energy balance. The spectral observations allow for the delineation of clearly differentiated radiative regimes according to snowpack thickness, showing that centimeter-scale variations in snow cover induce abrupt changes in spectral albedo. The transition toward exposed ice surfaces is characterized by a pronounced reduction in albedo, underscoring the critical importance of surface state in the radiative response of the glacier surface.

The observed spectral albedo was compared with BioSNICAR simulations obtained using the PO configuration, constrained by the surface properties measured in the field and the in situ eBC concentrations, both without and with the inclusion of MD (Fig. 5). The comparison reveals clear differences among glacier surface states, both in albedo magnitude and spectral structure. For CS (Fig. 5a–c), the PO configuration generally reproduces the observed spectral structure in the near-infrared and shortwave region ($\lambda > 1$ μm), where the optical response is strongly controlled by the structure and scattering properties of the snowpack. In contrast, the largest discrepancies occur at shorter wavelengths, particularly in the visible range, where the observed albedo is generally lower than simulated. The inclusion of MD shifts the simulated albedo toward the observations and reduces these discrepancies, although the agreement is not uniform across the spectral range. This behavior indicates that the configuration constrained by the measured snow properties and eBC alone does not fully reproduce the spectral absorption observed over continuous snow surfaces.

TS surface (Fig. 5d–f) exhibits a more heterogeneous response. In Fig. 5d, the inclusion of MD improves the agreement between simulated and observed spectra, whereas in Figs. 5e–f the PO and MD simulations are nearly indistinguishable, as no additional MD contribution is required in these cases. This variability occurs across a surface state characterized by reduced snow thickness and an increasing influence of the underlying ice on the surface optical response. For IE (Fig. 5g–i), differences between the observations and the PO configuration are again evident, particularly at shorter wavelengths, while the inclusion of MD brings the simulations closer to the observed spectra, although the magnitude of the inferred contribution varies among samples. Figure 5 shows that mineral dust accounts for part of the absorption that remains underestimated by the eBC-constrained PO configuration, but does not generally eliminate the differences between simulated and observed spectra. The persistence of these discrepancies with their variation among surface states, indicates that the observed optical response cannot be fully described by snow and ice physical properties, eBC, and MD alone, motivating the evaluation of additional optically active constituents through the bio-optical parameterizations.

https://doi.org/10.5194/egusphere-2026-5535
Preprint. Discussion started: 22 November 2026
© Author(s) 2026. CC BY 4.0 License.

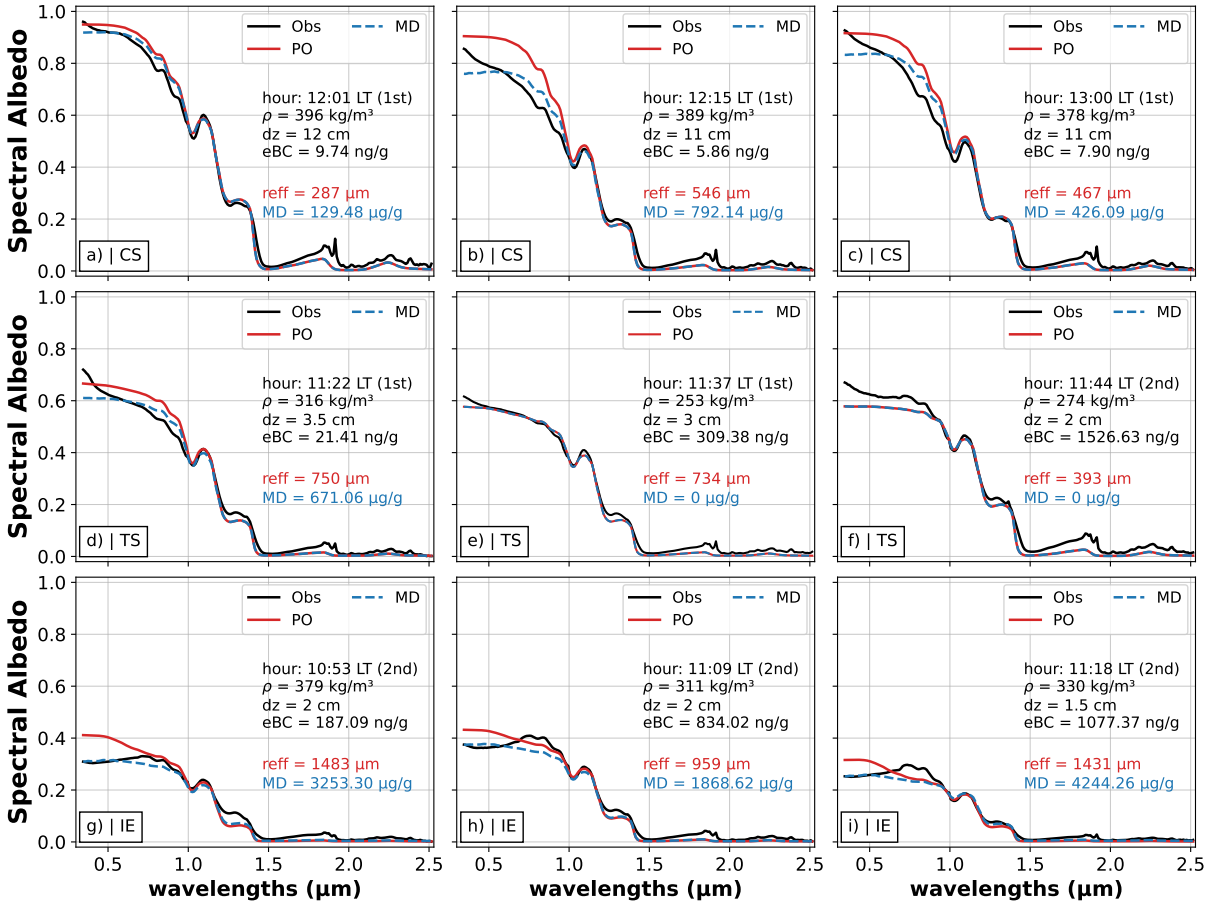


Figure 5. Comparison between observed spectral albedo (Obs) and BioSNICAR simulations using the physical-optical (PO) configuration constrained by observed parameters, with and without mineral dust (MD), for the glacier surface types shown in Fig. 4.

Figure 6 compares the observed spectral albedo with BioSNICAR simulations incorporating the COOK and CHEV bio-optical parameterizations. These simulations build on the conditions considered in Figure 5, including the contribution of mineral dust, and allow the spectral response to be evaluated after introducing biological components. Both parameterizations reproduce the main spectral features observed across the three surface states, particularly in the visible range ($\lambda < 1$ μm), where the largest differences between the physical-optical simulations and observations occur. The improvement relative to the simulations including eBC and mineral dust is most evident in the magnitude and shape of absorption at shorter wavelengths, although the response varies among surface states.

For CS surfaces (Fig. 6a–c), both parameterizations reproduce the structure of the observed spectra, including the decrease in albedo toward shorter wavelengths. The main differences between COOK and CHEV occur at the shorter-wavelength end of the spectrum and between approximately 0.75 and 1 μm, where COOK generally provides a closer fit to the observed albedo than CHEV. This indicates that the choice of bio-optical parameterization influences the representation of the spectral response

https://doi.org/10.5194/egusphere-2026-5535
Preprint. Discussion started: 22 November 2026
© Author(s) 2026. CC BY 4.0 License.

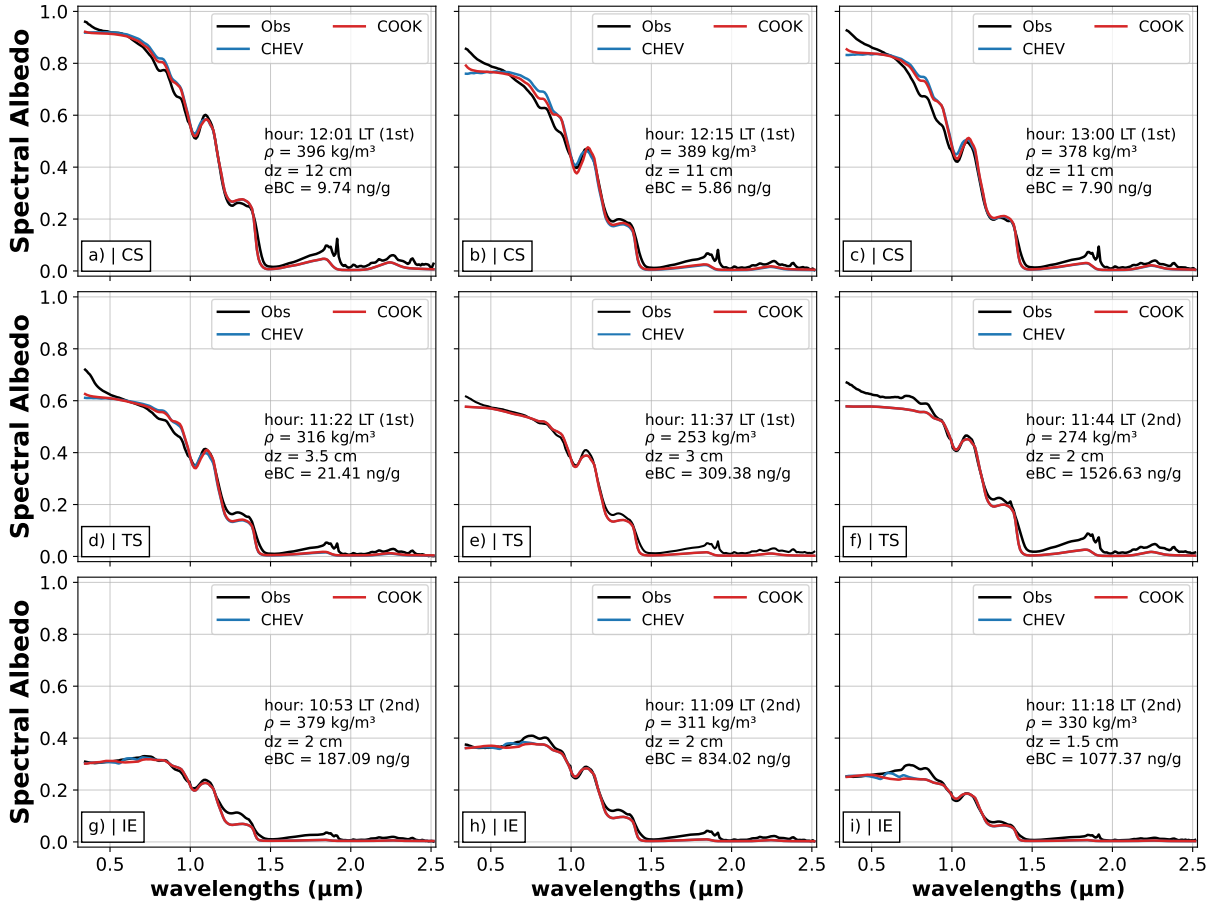


Figure 6. Observed spectral albedo and BioSNICAR simulations using the COOK and CHEV bio-optical parameterizations, including MD and biological impurities, for the glacier surface types shown in Fig. 4

of continuous snow, particularly in spectral regions sensitive to impurity absorption. In the near-infrared, the simulated spectra remain closely associated with the optical properties of the snowpack, although differences in albedo magnitude persist between the parameterizations.

For TS surfaces (Fig. 6d–f), COOK and CHEV produce broadly similar spectral responses and reproduce the main features of the observed signal. The differences between the parameterizations are smaller than those observed for CS surfaces, although COOK still shows a somewhat closer agreement with the observations in the same spectral regions. The agreement is particularly close around the spectral transitions near 1 and 1.3 μm. This intermediate behavior is consistent with the reduced snow cover, which progressively modifies the optical contribution of the snowpack and increases the influence of the underlying ice.

For IE surfaces (Fig. 6g–i), both parameterizations reproduce the main characteristics of the observed spectra, including the low albedo and the spectral transitions toward the near-infrared. In contrast to CS and TS surfaces, CHEV provides a closer fit to the observations around 0.6 μm than COOK. Although differences between the parameterizations are relatively

https://doi.org/10.5194/egusphere-2026-5535
Preprint. Discussion started: 22 November 2026
© Author(s) 2026. CC BY 4.0 License.

localized, this result indicates that their relative performance changes as the surface transitions from snow-covered to exposed-ice conditions. The bio-optical parameterizations therefore contribute differently to the representation of the observed spectral response depending on the optical state of the surface, complementing the effects associated with mineral dust.

The effect of mineral dust was quantified by comparing the spectral fits obtained with the physical-optical configuration constrained by the measured eBC concentrations, with and without the inclusion of MD (Table 1). The inclusion of MD reduces the MAE for most samples, although the magnitude of the improvement varies among surface states. For continuous snow, the reduction is consistent across all three samples, with MAE decreasing from $0.02 - 0.047$ to $0.021 - 0.025$. For exposed ice, MD reduces the MAE in four of the six samples, while no additional MD contribution is required for the remaining two cases.

The changes in BBA are also consistent with the spectral adjustments obtained after including MD. In cases where MD improves the spectral fit, the simulated BBA generally shifts toward the observed values, indicating that its effect extends beyond localized changes in spectral shape to the integrated shortwave reflectance. These results quantitatively confirm the behavior observed in Fig. 5: measured eBC concentrations alone are insufficient to reproduce the observed spectral albedo, while mineral dust accounts for an additional fraction of the surface absorption. However, the absence of an MD contribution in some transitional-snow cases and the remaining spectral differences indicate that mineral dust does not fully account for the observed optical response.

The combined LAPs simulations show that the composition associated with the best spectral fits varies systematically with surface state and bio-optical parameterization (Table 2). For CS conditions, particularly at greater snow depths, COOK consistently exhibits a lower MAE than CHEV across all samples, indicating a better statistical fit to the observed albedo spectra. Moreover, snow algae are more frequently identified among the LAP compositions associated with the best-fitting COOK simulations. In contrast, CHEV more frequently favours compositions including MD and ice algae. Thus, COOK performs better for continuous and relatively thick snow surfaces, with the spectral fits providing evidence consistent with a contribution from snow algae. Despite differences in the inferred LAP compositions, several combinations can produce comparable spectral responses, highlighting the non-uniqueness of spectral albedo inversion.

For IE conditions, including surfaces with low snow depth, the relative performance of the parameterizations reverses. CHEV generally yields lower MAE values than COOK, indicating a better statistical fit to the observed spectra under exposed-ice conditions. In these cases, MD and ice algae occur more frequently among the LAP compositions associated with the best-fitting simulations, whereas snow algae are less prevalent. The recurrence of MD and ice algae in the best-fitting CHEV simulations suggests that these impurities contribute more strongly to the observed optical properties of the ablation-zone surface. Indicate a transition in the LAPs composition associated with the best spectral fits as the glacier surface evolves from continuous, relatively thick snow toward low-snow-depth and exposed-ice conditions COOK performs better for continuous snow and is more frequently associated with snow algae, whereas CHEV performs better for exposed ice and is more frequently associated with MD and ice algae.

https://doi.org/10.5194/egusphere-2026-5535
Preprint. Discussion started: 22 November 2026
© Author(s) 2026. CC BY 4.0 License.

Table 1. BioSNICAR simulations using a base physical-optical configuration and the same configuration with mineral dust added. Both simulations were forced with in situ measured glaciological parameters and eBC concentrations. Model performance was evaluated using the mean absolute error (MAE) and broadband albedo (BBA) relative to the observed spectral albedo.

dz (cm)	Density (kg m^{-3})	reff (μm)	**Physical-optical**			**Mineral dust**		
			eBC (ng g^{-1})	MAE	BBA	Dust (μg kg^{-1})	MAE	BBA
12.0	396	287	9.74	0.025	0.722	129.48	0.021	0.705
11.0	389	546	5.86	0.047	0.668	792.14	0.024	0.583
11.0	378	467	7.90	0.034	0.685	426.09	0.025	0.636
3.5	316	750	21.41	0.025	0.502	671.06	0.019	0.468
3.0	253	734	309.38	0.014	0.439	0	0.014	0.439
1.5 $\pm$ 1	271	655	306.30	0.018	0.433	0	0.018	0.433
1.0 $\pm$ 1	379	1483	187.09	0.026	0.292	3253.30	0.014	0.243
0.5 $\pm$ 1	387	1180	217.01	0.017	0.184	24809.26	0.013	0.171
1.0 $\pm$ 1	311	959	834.02	0.020	0.322	1868.62	0.017	0.292
0.5 $\pm$ 1	330	1431	1077.37	0.017	0.222	4244.26	0.012	0.199
1.0 $\pm$ 1	274	393	1526.63	0.029	0.463	0	0.029	0.463

3.3 Factors influencing surface albedo and radiative forcing

Figure 7 summarizes the relationships between BBA and the physical properties and light-absorbing constituents of the glacier surface. The strongest relationships are found with the physical properties of the snowpack. Snow depth (dz) shows a strong positive relationship with BBA ($r^2 = 0.795$; Fig. 7a), whereas effective grain radius (r_{eff}) exhibits a strong negative relationship ($r^2 = 0.767$; Fig. 7b). These relationships indicate that the broadband optical response is closely associated with the physical state of the snowpack. Thicker snow layers are associated with higher BBA, consistent with enhanced multiple scattering and a reduced influence of the darker underlying ice, whereas larger effective grain sizes are associated with lower BBA, consistent with reduced scattering efficiency and enhanced absorption during snow metamorphism.

https://doi.org/10.5194/egusphere-2026-5535
Preprint. Discussion started: 22 November 2026
© Author(s) 2026. CC BY 4.0 License.

Table 2. BioSNICAR simulations using the base PO configuration with the (CHEV and COOK) bio-optical parameterizations, incorporating mineral dust, snow algae, and ice algae, with the additional LAPs concentrations adjusted to the observed spectral albedo. Biological impurity concentrations are reported in the parameterization-specific units used by CHEV and COOK and are not directly comparable between parameterizations.

dz (cm)	CHEV					COOK				
	Mineral dust (μg kg^{-1})	Snow algae (cells mL^{-1})	Ice algae (cells mL^{-1})	MAE	BBA	Mineral dust (μg kg^{-1})	Snow algae (ng g^{-1})	Ice algae (cells mL^{-1})	MAE	BBA
12.0	130	0	0	0.021	0.722	0	260000	0	0.019	0.722
11.0	790	0	0	0.024	0.610	0	1280000	0	0.020	0.611
11.0	430	0	0	0.025	0.685	0	680000	0	0.022	0.662
3.5	670	0	0	0.019	0.471	0	790000	0	0.017	0.489
3.0	0	0	0	0.014	0.439	0	0	0	0.014	0.439
1.5 $\pm$ 1	0	0	0	0.018	0.433	0	0	0	0.018	0.433
1.0 $\pm$ 1	1220	170000	80000	0.011	0.276	1260	0	190000	0.012	0.276
0.5 $\pm$ 1	0	520000	80000	0.008	0.160	60	0	420000	0.009	0.184
1.0 $\pm$ 1	0	200000	90000	0.012	0.322	0	0	220000	0.013	0.322
0.5 $\pm$ 1	360	360000	0	0.011	0.222	800	0	220000	0.012	0.220
1.0 $\pm$ 1	0	0	0	0.029	0.463	0	0	0	0.029	0.463

The relationships with surface impurities are comparatively weaker and differ among impurity types. Algal abundance shows a negative relationship with BBA ($r^2 = 0.410$; Fig. 7d), similar to the relationship reported by Chevrollier et al. (2023) for cryospheric environments. In contrast, the relationships with MD and eBC are weak ($r^2 = 0.163$ and 0.159, respectively; Fig. 7e–f). The stronger association between BBA and algal abundance relative to MD and eBC suggests that biological impurities may contribute to broadband albedo variability at the glacier surface. However, these bivariate relationships do not by themselves establish causality or allow the relative radiative effects of individual LAPs to be separated, particularly given the covariation among surface properties and impurity concentrations.

SZA shows a moderate positive relationship with BBA ($r^2 = 0.522$; Fig. 7c). A lower SZA places the incident solar radiation closer to the zenith of the glacier, reducing the dispersion of incoming irradiance, whereas a higher SZA increases irradiance dispersion and is associated with higher BBA. Similarly, lower SZA and reduced irradiance dispersion are associated with snow and ice melting, reflected in lower snow depth and greater eBC accumulation at the surface (Fig. 7g–h). SZA covaries with eBC concentration ($r^2 = 0.673$; Fig. 7g) and snow depth ($r^2 = 0.534$; Fig. 7h), linking solar geometry with the evolving surface conditions. The negative relationship between dz and r_{eff} ($r^2 = 0.432$; Fig. 7i) further shows that larger effective grain sizes are associated with thinner snow cover, consistent with snow aging.

https://doi.org/10.5194/egusphere-2026-5535
Preprint. Discussion started: 22 November 2026
© Author(s) 2026. CC BY 4.0 License.

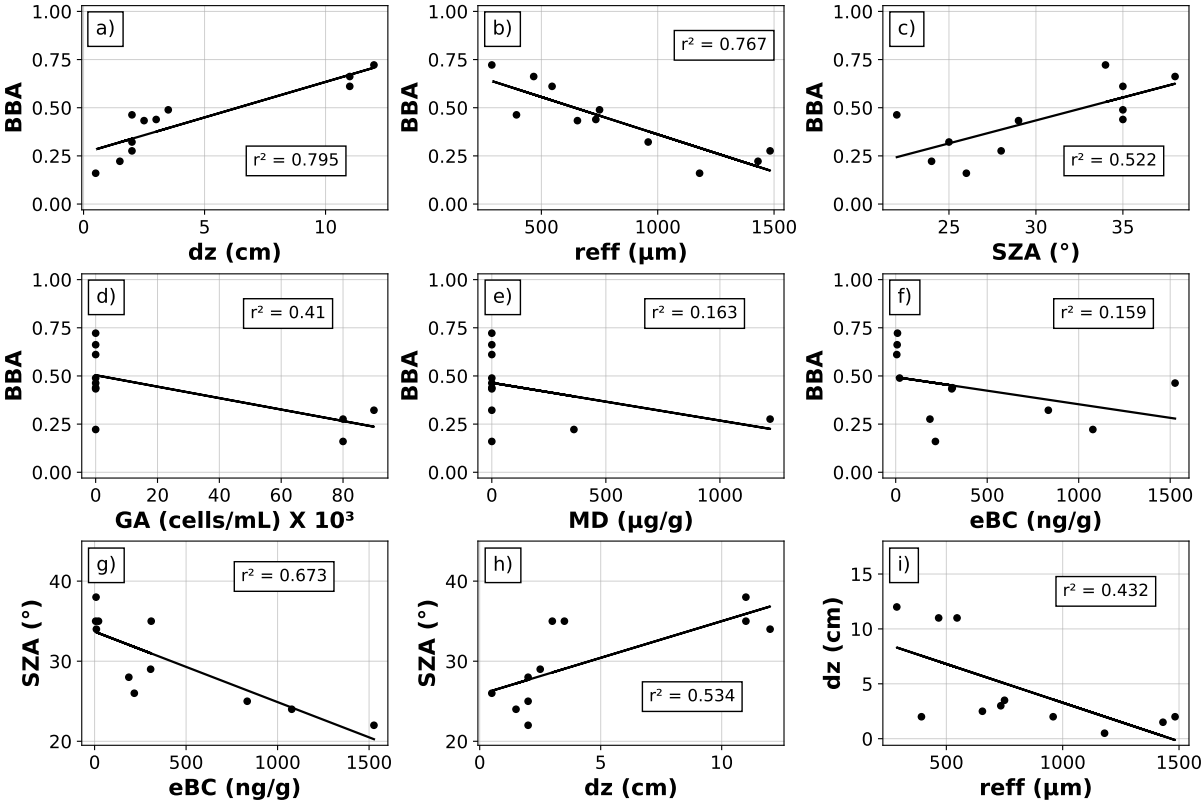


Figure 7. Relationships between broadband albedo (BBA) and snow physical properties, surface impurity concentrations, and solar zenith angle (SZA).

The observed variability in BBA is more strongly associated with snow physical properties, particularly dz and r_{eff}, than with the concentration of any individual LAPs. At the same time, the relationship with algal abundance provides an independent indication that biological impurities may be relevant to the broadband optical response, complementing the spectral evidence obtained from the BioSNICAR simulations. These relationships therefore support an interpretation of glacier-surface albedo in which the optical effect of LAPs is modulated by the evolving physical state of the snow and ice surface rather than by impurity concentration alone.

Radiative forcing exhibited pronounced interannual and intra-seasonal variability throughout the analyzed period (2022-2026) (Fig. 8), with significant differences in both magnitude and timing of peak values. The highest and most abrupt peaks are observed in 2023, 2024, and 2025; however, these maxima do not occur in the same months, indicating that extreme radiative forcing events are not strictly controlled by seasonality, but rather by variable surface conditions of the glacier system. In 2024, elevated radiative forcing values are observed during the wet-season months (March-April, 8), which is particularly notable given that higher albedo conditions are typically expected due to snow presence. This behavior is consistent with the albedo

https://doi.org/10.5194/egusphere-2026-5535
Preprint. Discussion started: 22 November 2026
© Author(s) 2026. CC BY 4.0 License.

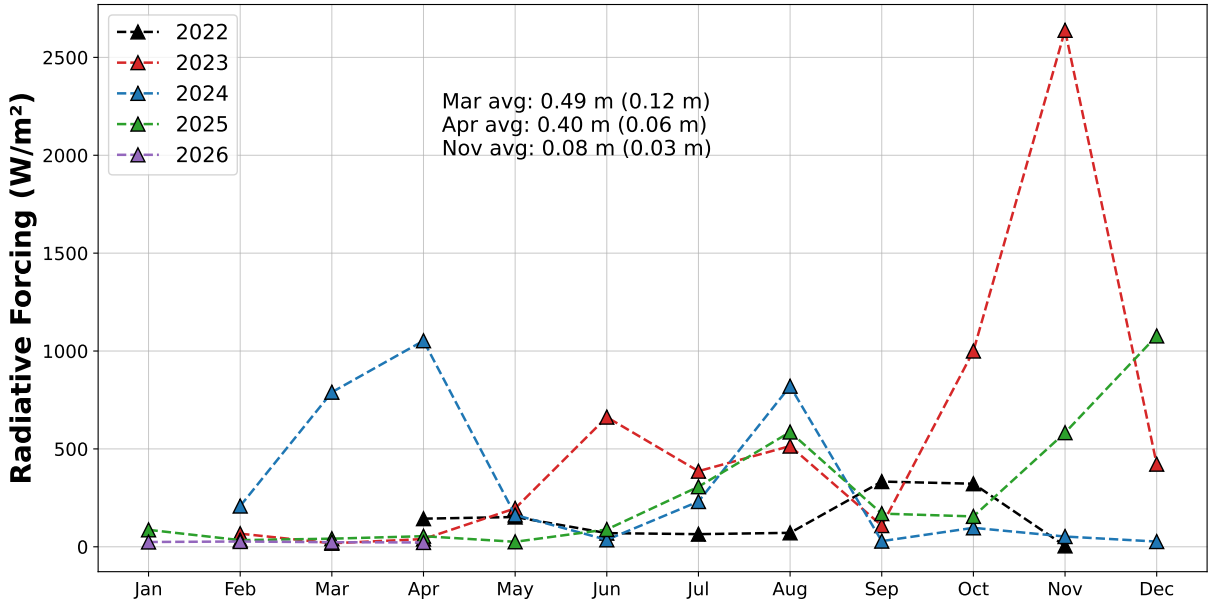


Figure 8. Monthly radiative forcing (Wm^2) for 2022-2026, showing strong interannual variability and shifts in the timing of peak values.

dynamics shown in Figure 3, where critically low albedo values were recorded during the same period, suggesting reduced snow persistence and increased exposure of impurity-enriched surfaces.

The anomalous values observed at the end of 2023 and beginning of 2024 (Fig. 8) are particularly relevant in the context of the 2023-2024 El Niño event. These periods were characterized by strongly anomalous eBC concentrations, associated with reduced snow persistence and the re-exposure of impurity-enriched glacier surfaces. Thus, the elevated eBC signal likely reflects not only atmospheric inputs but also the re-exposure and accumulation of previously deposited carbonaceous impurities as snow cover diminished, enhancing shortwave radiation absorption. In contrast, the anomaly observed in December 2025 (Fig. 8) may be related primarily to short-term glacier-surface dynamics, although the occurrence of a short-lived dry spell, characterized by a precipitation deficit during this month, may also have contributed to the anomalous response. Apart from these anomalous periods, the radiative forcing values remain broadly consistent with a seasonal pattern of higher forcing between the dry season and the first months of transition toward the wet season.

In contrast, other years such as 2023 and 2025 exhibit peak radiative forcing during the dry season (July-November), when snow cover is minimal or absent. Under these conditions, the glacier surface is dominated by exposed ice surfaces and higher concentrations of LAPs, leading to reduced albedo and enhanced shortwave radiation absorption. The results indicate that years characterized by limited snow accumulation or persistence exhibit more intense and frequent radiative forcing events. This highlights the key role of snow cover as a regulator of surface albedo and demonstrates that the absence or rapid depletion of snow increases the sensitivity of the glacier surface to processes of surface darkening. Consequently, radiative forcing in tropical glaciers is highly variable and primarily controlled by short-term changes in surface state and impurity presence.

https://doi.org/10.5194/egusphere-2026-5535
Preprint. Discussion started: 22 November 2026
© Author(s) 2026. CC BY 4.0 License.

eBC exhibited distinct relationships with melt rate (Mm, $w.e.\ d^{-1}$) under CS and IE conditions (Fig. 9). In both cases, a positive and non-linear relationship is observed, indicating that increasing eBC concentrations enhance surface melt. This highlights the direct role of light-absorbing impurities in modulating melt processes through radiative forcing. Melt rates reach up to 0.53 cm w.e. d^1 under CS conditions and 0.13 cm $w.e.\ d^{-1}$ under IE conditions, indicating that the CS configuration is approximately four times more sensitive to BC-induced forcing. The stronger response under snow-covered conditions reflects the higher sensitivity of snow albedo to impurity loading. The observed nonlinear behavior suggests a progressive reduction in marginal impact at higher eBC concentrations, consistent with albedo saturation effects and radiative shielding within the snowpack. The system response is significantly more sensitive under snow-covered conditions, where small increases in eBC concentration result in pronounced increases in meltwater. This is because snow initially exhibits high albedo; thus, the incorporation of LAPs efficiently reduces surface reflectivity and substantially enhances shortwave radiation absorption. In contrast, under IE conditions, the sensitivity of Mm to increasing eBC is lower. This reflects the fact that ice already has a relatively low albedo, so the additional effect of impurities on radiative absorption is more limited compared to snow surfaces. Furthermore, the non-linear shape of the curves suggests that the impact of eBC is more pronounced at low to intermediate concentration ranges, with a progressively weaker response at higher concentrations. This behavior indicates a partial saturation of the darkening effect, where further reductions in albedo become less efficient as the surface approaches optically darker states.

These results highlight the strong sensitivity of the glacier surface to changes in surface state and impurity loading, as reflected in both the variability of radiative forcing and the response of the surface melt. Periods characterized by reduced snow cover and increased concentrations of LAPs correspond to conditions of enhanced radiative absorption and amplified mass loss. This behavior demonstrates that the impact of impurities on glacier melt is not solely dependent on their concentration, but on their interaction with the prevailing surface conditions, particularly the presence or absence of snow. As a result, transitions between snow-covered and ice-exposed states emerge as critical controls on the magnitude of radiative forcing and its translation into surface mass loss.

4 Discussion

4.1 Atmosphere-snowpack coupling and impurity variability

The observational and modeling data allowed understanding the coupling between atmospheric forcing and the glacier surface response, integrating eBC concentrations with the evolution of albedo and the physical state of the snowpack in a tropical high-mountain environment. This observational framework is particularly relevant given the transient nature of these systems, where processes of deposition, redistribution, and exposure of impurities occur over short spatiotemporal scales. The representativeness of eBC in snow is conditioned by its high spatial variability and by the discontinuity of snow cover throughout the year, which restricts direct comparability between campaigns. During advanced stages of ablation, snow scarcity induces a systematic shift of sampling toward higher elevations within the ablation zone. The acquisition of continuous monthly series constitutes an operational challenge inherent to tropical glaciers. These limitations highlight the need to strengthen systematic

https://doi.org/10.5194/egusphere-2026-5535
Preprint. Discussion started: 22 November 2026
© Author(s) 2026. CC BY 4.0 License.

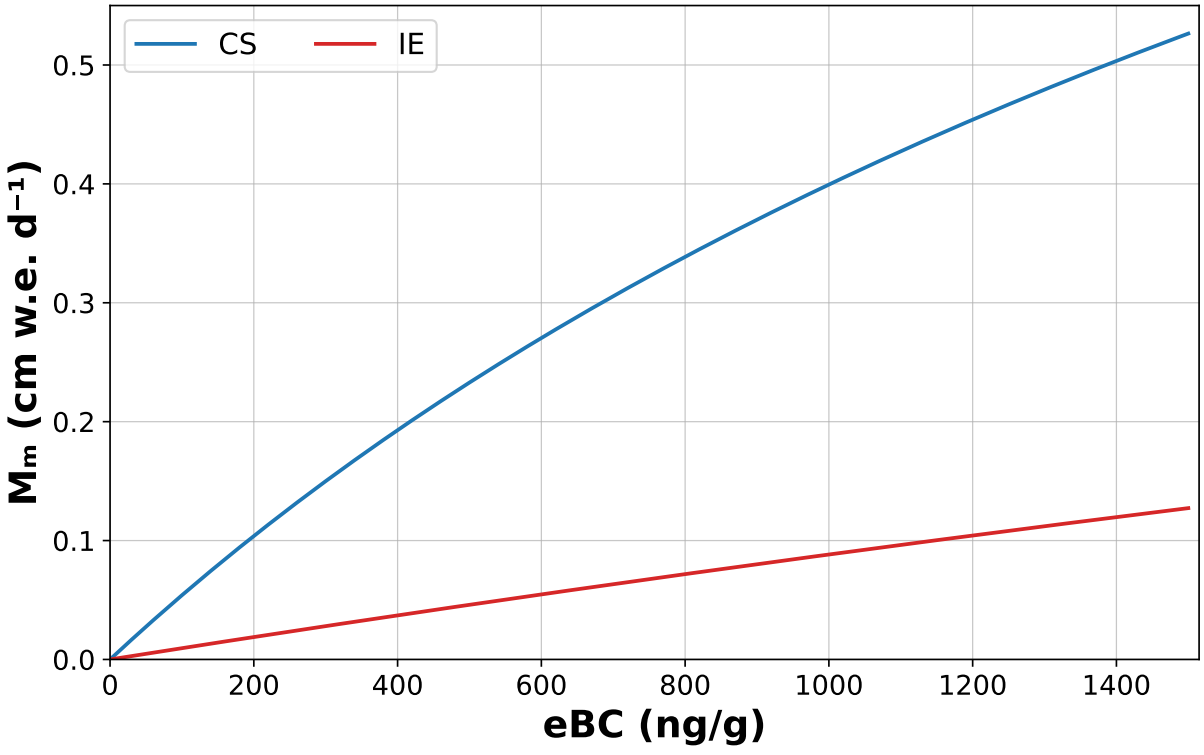


Figure 9. Daily eBC-induced melt mass (M_m) as a function of eBC for two conditions, continuous snow(CS) and ice-exposed surfaces (IE)

monitoring of LAPs in glaciers and to advance in the standardization of measurement protocols (Ontiveros-Gonzalez et al., 2025), which will improve the consistency and comparability of observations in the Andean cryosphere. Nevertheless, the coherence between atmospheric eBC variability, the physical properties of the snowpack, spectral albedo, and the surface radiative response supports a physically consistent interpretation of the dominant processes, backed by direct observational evidence. A strong but non-linear coupling is identified between atmospheric eBC, snowpack evolution, and its surface concentration. Although the seasonal maximum of atmospheric eBC during the dry season (July–November) translates into an increase in surface concentrations, the occurrence of high values during the wet season (Fig. 2a) shows that the impurity load does not respond exclusively to immediate atmospheric forcing. This behavior indicates that, although there is coupling at the seasonal scale, the surface response exhibits a temporal decoupling associated with internal snowpack processes. In particular, the reduction of snow depth favors the progressive concentration of previously deposited impurities due to ablation, generating an effective amplification of surface eBC independent of contemporaneous deposition. The inverse relationship between snow depth and eBC concentration further suggests that the glacier surface acts as a transient reservoir of impurities, where processes of accumulation and re-exposure modulate the surface signal. This behavior is particularly relevant for tropical glaciers, where shallow and highly dynamic snowpacks can modify the surface expression and radiative contribution of deposited LAPs. Previous studies have shown that the radiative effect of mineral dust can be smaller than that of black carbon under specific

https://doi.org/10.5194/egusphere-2026-5535
Preprint. Discussion started: 22 November 2026
© Author(s) 2026. CC BY 4.0 License.

glacier and snowpack conditions (Gabbi et al., 2015; Weber et al., 2026). Our results are consistent with this interpretation, while also showing that mineral dust contributes to the observed spectral response under the conditions investigated here. Its inclusion in the eBC-constrained PO configuration reduces the spectral fitting error for most samples, although the magnitude of the improvement varies with surface state and MD alone does not fully reproduce the observed spectra. The remaining discrepancies therefore motivate the consideration of additional optically active constituents, including biological impurities in the representation of glacier surface albedo.

4.2 Albedo-impurity feedback

The results show that the LAP-induced albedo feedback operates at the sub-seasonal scale; this process intensifies under conditions of advanced ablation, where the thinning of the snowpack favors an increasing influence of surface impurities on the optical response. In this regime, the reduction of albedo and the increase in energy absorption respond to a coupling between the surface state and the LAPs load, in which small variations in snow thickness generate disproportionate changes in radiation absorption. This behavior is consistent with the albedo–ablation feedback mechanism described in mid-latitude glaciers (Gabbi et al., 2015), but in the present study it manifests under conditions of high snowpack transience, where snow persistence controls the activation or inhibition of this process. In addition, in line with recent studies (Saito et al., 2026), albedo emerges as the main modulator of melt energy; however, our results show that this modulation is conditioned by the interaction between LAPs loading and the evolution of the surface state, which positions this coupling as an important control of the surface radiative response at sub-seasonal timescales.

Likewise, the spectral analysis shows a direct dependence of surface albedo on snowpack thickness, with well-defined transitions between conditions of continuous snow, thin snow, and exposed ice. Thin snow conditions emerge as a critical state, since, despite the presence of snow, the combination of low thickness and high impurity concentration produces a significant reduction in albedo ($BBA \approx 0.56$), which shows that optically thin layers are not effective in isolating the underlying ice. This favors the penetration of solar radiation and its absorption in deeper layers (Warren, 2019). As snow thickness decreases, the optical influence of the underlying glacier ice progressively increases, so that the radiative effect of LAPs is expressed within an evolving snow–ice optical system rather than over a fixed surface. Consequently, the same impurity load can produce different spectral and radiative responses depending on whether it is embedded in continuous snow, a thin snow layer, or a predominantly exposed-ice surface. These results show that centimeter-scale variations in snow thickness generate abrupt changes in spectral albedo, reinforcing the role of the surface state as a primary control of the radiative response.

4.3 Sub-seasonal variability and modeling

The temporal analysis shows that surface albedo responds highly sensitively to short-scale atmospheric variability, particularly to the interaction between BC load and solid precipitation events. In this study, snowfall events are observed to induce efficient removal of eBC through wet deposition, establishing a direct link between atmospheric variability and the redistribution of impurities on the glacier surface. In contrast, periods with high atmospheric load and scarce snow cover generate rapid decreases in albedo, reflecting an immediate surface response to dominant atmospheric conditions. This high intra-seasonal variability

https://doi.org/10.5194/egusphere-2026-5535
Preprint. Discussion started: 22 November 2026
© Author(s) 2026. CC BY 4.0 License.

is consistent with the transient nature of the snowpack in tropical glaciers, where the alternation between accumulation and ablation occurs over short timescales, making a purely seasonal classification insufficient (Fyffe et al., 2025). The results show that sub-seasonal fluctuations in albedo are closely coupled to atmospheric variability, modulating the glacier surface response (Gurgiser et al., 2013; Saito et al., 2026).

Snowfall events temporarily restore high-reflectance conditions, acting as a transient mechanism of surface renewal. However, this effect is short-lived, as subsequent ablation rapidly reduces snow cover and exposes ice surfaces enriched in impurities. Under these conditions, even during the wet season associated with elevated albedo values, a stable radiative regime is not established. Periods of several days without solid precipitation favor a rapid reduction of the snowpack and abrupt decreases in albedo toward values comparable to those of the dry season, configuring an efficient mechanism of exposure and concentration of impurities at seasonal and sub-seasonal scales.

Previous studies in tropical Andean glaciers have emphasized the role of snowfall in maintaining high-albedo surface conditions and regulating melt through periodic snow-cover renewal (Sicart et al., 2011; Gurgiser et al., 2013; Rabatel et al., 2013). Our observations suggest that the glacier radiative response is influenced not only by the occurrence of snowfall events but also by the persistence of snow cover following deposition. The close correspondence between snow depth and albedo with the observed altitudinal snow-persistence gradient, indicates that snow-cover duration exerts an important control on the timing of transitions from snow-covered to IE conditions across the glacier. These observations provide direct evidence that variations in snow-cover persistence strongly influence glacier radiative conditions at intraseasonal scales and contribute to the marked spatial and temporal heterogeneity observed in glacier albedo.

The comparison between observed spectral albedo and that simulated with BioSNICAR reveals systematic limitations in the representation of the optical properties of the glacier surface under the physico-optical configuration, where persistent discrepancies are observed in the visible and ultraviolet range, indicating an underestimation of radiative absorption. These differences show that, even when forcing the model with in situ measured eBC concentrations, the physico-optical configuration does not fully capture the contribution of all optically active components present at the surface. In particular, the greater absorption observed in the visible with the improvement in spectral representation when incorporating bio-optical configurations (COOK and CHEV), indicates that additional absorbing constituents contribute to the observed albedo variability, in agreement with previous studies (Cook et al., 2017; Chevrollier et al., 2023).

The additional simulations with mineral dust and biological impurities provide further constraints on this interpretation. Mineral dust improves the spectral representation for most samples, confirming that eBC alone does not account for the full observed absorption. However, the combined LAPs simulations show that the inferred contribution depends on surface state and bio-optical parameterization. For continuous snow, COOK provides the most consistent representation, achieving equal or lower fitting errors across the analyzed samples and more frequently favouring snow algae, whereas CHEV more frequently favours mineral dust and ice algae. The fact that different combinations of LAPs can produce comparable spectral fits indicates that the observations constrain the integrated optical effect of the impurities more strongly than the contribution of any single component. Although both parameterizations can reproduce the observed spectra, COOK provides the most consistent performance across snow-dominated surfaces, supporting its use for continuous snow. In exposed ice, CHEV shows comparable or

https://doi.org/10.5194/egusphere-2026-5535
Preprint. Discussion started: 22 November 2026
© Author(s) 2026. CC BY 4.0 License.

slightly stronger performance in reproducing the observed spectra, while ice-algae parameterizations recur among the best-fitting cases under both approaches. These results indicate that the relative performance of the bio-optical parameterizations depends strongly on surface state, with COOK showing greater consistency for continuous snow and CHEV being particularly relevant under exposed-ice conditions. Nevertheless, the differences between the two parameterizations for exposed ice are small, and neither shows a clear advantage. The recurrence of ice algae among the best-fitting cases under both parameterizations with the variability in the contributions of mineral dust and snow algae, indicates that biological impurities contribute to the spectral response beyond the effect of mineral dust alone. This behaviour is consistent with Di Mauro et al. (2024), who showed that mineral dust and snow algae can produce overlapping spectral effects and that their combined radiative influence is not necessarily additive. These results highlight the importance of considering multiple LAPs when interpreting spectral albedo on tropical glacier surfaces.

The results show that the eBC-induced melt-equivalent response differs between surface states, being approximately four times higher under CS conditions than under IE. This contrast indicates that the radiative effect of black carbon depends on the thickness and persistence of the snowpack. During wet removal episodes, the coincidence of atmospheric BC decreases with precipitation events indicates conditions favourable for BC transfer to the snow surface, increasing radiation absorption and potentially accelerating melt, in agreement with what has been reported in tropical Andean glaciers (Bonilla et al., 2023). Thus, the contribution of eBC to surface energy absorption is not determined by atmospheric loading alone, but also by the capacity of the underlying surface to absorb additional shortwave radiation.

5 Conclusions

Based on in situ observational data and radiative transfer simulations obtained over a five-year period (2022-2026) on a tropical glacier in the central Andes of Peru, this study provides an integrated characterization of the physical mechanisms controlling surface albedo variability and its impact on shortwave radiation absorption. The results indicate that the interaction between snowpack dynamics, LAPs deposition, and atmospheric variability modulates the energy available for melt, highlighting the role of albedo as a non-linear integrative variable of the glacier system, linking atmospheric forcing, transient snow cover, and impurity deposition.

- The transient nature of the snowpack leads to rapid transitions between snow-covered states and exposed ice surfaces, producing abrupt changes in albedo and radiative forcing. These transitions occur even during the wet season, indicating that this period does not constitute a stable radiative regime and may exhibit episodes of high absorption associated with rapid surface state evolution. This behavior suggests that mass balance models may underestimate melt variability if they do not explicitly represent albedo evolution and impurity dynamics.

- LAPs exhibit a marked seasonal signal; however, its radiative impact is controlled by snowpack evolution. Snow thinning and impurity re-exposure promote surface enrichment, activating a LAP-induced albedo–impurity feedback mechanism that amplifies radiative absorption and partially decouples the surface response from immediate atmospheric forcing.

https://doi.org/10.5194/egusphere-2026-5535
Preprint. Discussion started: 22 November 2026
© Author(s) 2026. CC BY 4.0 License.

This effect is non-linear, with higher sensitivity under snow-covered conditions, where the radiative forcing efficiency of BC is maximized, and decreases as the surface evolves toward lower-albedo states.

– The spectral albedo simulations show that eBC alone is insufficient to reproduce the observed absorption, whereas the inclusion of mineral dust improves the spectral representation, although it does not fully account for the observed spectra. The additional incorporation of biological components provides a more complete representation of the spectral signal. Comparison between the COOK and CHEV parameterizations reveals differences associated with surface state, COOK provides the most consistent representation for continuous snow, whereas CHEV provides a better representation over exposed ice, where ice algae recur among the best-fitting LAPs compositions. These results provide evidence that biological impurities may contribute to the observed surface optical signal and highlight the importance of considering biological impurities in the radiative characterization of tropical glaciers.

The results demonstrate that neglecting LAPs and their bio-optical components limits the representation of glacier surface optical properties, particularly in tropical glaciers where radiative response is strongly modulated by surface state. Their explicit inclusion is key to improving radiative forcing estimates and reducing uncertainties in glacier surface-energy-balance and melt modeling. Beyond these process-based findings, this study also provides, to our knowledge, the first in situ spectral albedo dataset for a tropical Andean glacier, offering an observational benchmark for future investigations of snow optics, radiative transfer, and glacier energy balance in the tropical Andes.

Data availability. The observational spectral albedo data are openly available at https://doi.org/10.5281/zenodo.22713881

Author contributions. EVP conceptualized the study, developed the methodology, conducted the field investigations, performed the formal analysis, and wrote the original manuscript. CV contributed to data curation and formal analysis of the field observations, conducted the radiative transfer simulations, and contributed to the visualization of the results. RM contributed to the review, editing, and scientific interpretation of the results. TC contributed to the initial development of the research proposal and to the review of the manuscript. CT supervised the acquisition of glaciological measurements and contributed to data curation of glacier albedo observations. FJ contributed to the investigation, methodology, and interpretation of the results. EC contributed to the acquisition, processing, and validation of the spectral measurements. BT contributed to project supervision, project administration, and review and editing of the manuscript.

Competing interests. The authors declare that they have no conflict of interest.

https://doi.org/10.5194/egusphere-2026-5535
Preprint. Discussion started: 22 November 2026
© Author(s) 2026. CC BY 4.0 License.



Acknowledgements. We thank Luis Suarez, David Guizado, Robinson Cuadros, and all colleagues who contributed to fieldwork and glacier expeditions in the Cordillera Huaytapallana. We also acknowledge the Black Carbon Project funded by PROCIENCIA (Contract No. PE501082856-2023), which supported the continuation of glacier monitoring in the region.

https://doi.org/10.5194/egusphere-2026-5535
Preprint. Discussion started: 22 November 2026
© Author(s) 2026. CC BY 4.0 License.

References

Bond, T. C., Doherty, S. J., Fahey, D. W., Forster, P. M., Berntsen, T., DeAngelo, B. J., Flanner, M. G., Ghan, S., Kärcher, B., Koch, D., et al.: Bounding the role of black carbon in the climate system: A scientific assessment, Journal of geophysical research: Atmospheres, 118, 5380–5552, https://doi.org/10.1002/jgrd.50171, 2013.

Bonilla, E., Mickley, L., Beaudon, E., Thompson, L., Rodriguez, W., Encarnación, R. C., Whicker, C., Flanner, M., Schmitt, C., and Ginot, P.: Contribution of biomass burning to black carbon deposition on Andean glaciers: consequences for radiative forcing, Environmental Research Letters, 18, 024 031, https://doi.org/10.1088/1748-9326/acb371, 2023.

Chen, J.-Z., Du, W.-T., Kang, S.-C., Qin, X., Sun, W.-J., Luo, L.-H., Li, Y., Yang, J.-H., and Jiang, Y.-Y.: Mitigation of black carbon emissions could immediately reduce 6.3% of glacier melting in the Qilian Mountains, Advances in Climate Change Research, 15, 725–736, https://doi.org/10.1016/j.accre.2024.06.010, 2024.

Chevrollier, L.-A., Cook, J. M., Halbach, L., Jakobsen, H., Benning, L. G., Anesio, A. M., and Tranter, M.: Light absorption and albedo reduction by pigmented microalgae on snow and ice, Journal of Glaciology, 69, 333–341, https://doi.org/10.1017/jog.2022.64, 2023.

Chevrollier, L.-A., Wehrlé, A., Cook, J. M., Pirk, N., Benning, L. G., Anesio, A. M., and Tranter, M.: Separating the albedo-reducing effect of different light-absorbing particles on snow using deep learning, The Cryosphere, 19, 1527–1538, https://doi.org/10.5194/tc-19-1527-2025, 2025.

Condom, T., Dumont, M., Mourre, L., Sicart, J. E., Rabatel, A., Viani, A., and Soruco, A.: A low-cost albedometer for snow and ice measurements–theoretical results and application on a tropical mountain in Bolivia, Geoscientific Instrumentation, Methods and Data Systems, 7, 169–178, https://doi.org/10.5194/gi-7-169-2018, 2018.

Cook, J. M., Hodson, A. J., Gardner, A. S., Flanner, M., Tedstone, A. J., Williamson, C., Irvine-Fynn, T. D., Nilsson, J., Bryant, R., and Tranter, M.: Quantifying bioalbedo: a new physically based model and discussion of empirical methods for characterising biological influence on ice and snow albedo, The Cryosphere, 11, 2611–2632, https://doi.org/10.5194/tc-11-2611-2017, 2017.

Cook, J. M., Tedstone, A. J., Williamson, C., McCutcheon, J., Hodson, A. J., Dayal, A., Skiles, M., Hofer, S., Bryant, R., McAree, O., et al.: Glacier algae accelerate melt rates on the south-western Greenland Ice Sheet, The Cryosphere, 14, 309–330, https://doi.org/10.5194/tc-14-309-2020, 2020.

Di Mauro, B., Garzonio, R., Ravasio, C., Orlandi, V., Baccolo, G., Gilardoni, S., Remias, D., Leoni, B., Rossini, M., and Colombo, R.: Combined effect of algae and dust on snow spectral and broadband albedo, Journal of Quantitative Spectroscopy and Radiative Transfer, 316, 108 906, https://doi.org/10.1016/j.jqsrt.2024.108906, 2024.

Doherty, S. J., Grenfell, T. C., Forsström, S., Hegg, D. L., Brandt, R. E., and Warren, S. G.: Observed vertical redistribution of black carbon and other insoluble light-absorbing particles in melting snow, Journal of Geophysical Research: Atmospheres, 118, 5553–5569, https://doi.org/10.1002/jgrd.50235, 2013.

Fierce, L., Bond, T. C., Bauer, S. E., Mena, F., and Riemer, N.: Black carbon absorption at the global scale is affected by particle-scale diversity in composition, Nature communications, 7, 12 361, https://doi.org/10.1038/ncomms12361, 2016.

Flanner, M. G., Zender, C. S., Randerson, J. T., and Rasch, P. J.: Present-day climate forcing and response from black carbon in snow, Journal of Geophysical Research: Atmospheres, 112, https://doi.org/10.1029/2006JD008003, 2007.

Flanner, M. G., Arnheim, J., Cook, J. M., Dang, C., He, C., Huang, X., Singh, D., Skiles, S. M., Whicker, C. A., and Zender, C. S.: SNICAR-AD v3: A community tool for modeling spectral snow albedo, Geoscientific Model Development Discussions, 2021, 1–49, https://doi.org/10.5194/gmd-14-7673-2021, 2021.

https://doi.org/10.5194/egusphere-2026-5535
Preprint. Discussion started: 22 November 2026
© Author(s) 2026. CC BY 4.0 License.

Fyffe, C. L., Potter, E., Fugger, S., Orr, A., Fatichi, S., Loarte, E., Medina, K., Hellström, R. Å., Bernat, M., Aubry-Wake, C., et al.: The energy and mass balance of Peruvian glaciers, Journal of Geophysical Research: Atmospheres, 126, e2021JD034 911, https://doi.org/10.1029/2021jd034911, 2021.

Fyffe, C. L., Potter, E., Miles, E., Shaw, T. E., McCarthy, M., Orr, A., Loarte, E., Medina, K., Fatichi, S., Hellström, R., et al.: Thin and ephemeral snow shapes melt and runoff dynamics in the Peruvian Andes, Communications Earth & Environment, 6, 434, https://doi.org/10.1038/s43247-025-02379-x, 2025.

Gabbi, J., Huss, M., Bauder, A., Cao, F., and Schwikowski, M.: The impact of Saharan dust and black carbon on albedo and long-term mass balance of an Alpine glacier, The Cryosphere, 9, 1385–1400, https://doi.org/10.5194/tc-9-1385-2015, 2015.

Gatti, L. V., Cunha, C. L., Marani, L., Cassol, H. L., Messias, C. G., Arai, E., Denning, A. S., Soler, L. S., Almeida, C., Setzer, A., et al.: Increased Amazon carbon emissions mainly from decline in law enforcement, Nature, 621, 318–323, https://doi.org/10.1038/s41586-023-06390-0, 2023.

Gilardoni, S., Di Mauro, B., and Bonasoni, P.: Black carbon, organic carbon, and mineral dust in South American tropical glaciers: A review, Global and Planetary Change, 213, 103 837, https://doi.org/10.1016/j.gloplacha.2022.103837, 2022.

Gurgiser, W., Marzeion, B., Nicholson, L., Ortner, M., and Kaser, G.: Modeling energy and mass balance of Shallap Glacier, Peru, The Cryosphere, 7, 1787–1802, https://doi.org/10.5194/tc-7-1787-2013, 2013.

Kang, S., Zhang, Y., Qian, Y., and Wang, H.: A review of black carbon in snow and ice and its impact on the cryosphere, Earth-science reviews, 210, 103 346, https://doi.org/10.1016/j.earscirev.2020.103346, 2020.

Li, Y.-J., Ding, Y.-J., Shangguan, D.-H., and Wang, R.-J.: Regional differences in global glacier retreat from 1980 to 2015, Advances in Climate Change Research, 10, 203–213, https://doi.org/10.1016/j.accre.2020.03.003, 2019.

Llactayo, V., Valdivia, J., Yarleque, C., Callañaupa, S., Villalobos-Puma, E., Guizado, D., and Alvarado-Lugo, R.: Future changes of precipitation types in the Peruvian Andes, Scientific Reports, 14, 22 634, https://doi.org/10.1038/s41598-024-71840-2, 2024.

Meng, L., Tu, L., Luo, J., Jiang, S., Ma, L., Cui, S., Yuan, Y., Zhou, J., Bian, Z., Jiang, Q., et al.: Anthropogenic Activities Increase the Proportion of Soot in Black Carbon Particles and Thereby Intensify Atmospheric Radiative Forcing, Environmental Science & Technology, 59, 15 159–15 169, https://doi.org/10.1021/acs.est.5c02892, 2025.

Niu, H., Kang, S., Wang, H., Du, J., Pu, T., Zhang, G., Lu, X., Yan, X., Wang, S., and Shi, X.: Light-absorbing impurities accelerating glacial melting in southeastern Tibetan Plateau, Environmental Pollution, 257, 113 541, https://doi.org/10.1016/j.envpol.2019.113541, 2020.

Ontiveros-Gonzalez, G., Carrillo, A., Davila, L., Muñoz, C., Calvo, D. K., Garcia, R., Rueda, L. F., et al.: Concentration of Black Carbon (BCe) in snow, glacier ice, and glacier water from high mountains in central Mexico and central Andes (Peru and Bolivia), Journal of South American Earth Sciences, p. 105668, https://doi.org/10.1016/j.jsames.2025.105668, 2025.

Rabatel, A., Francou, B., Soruco, A., Gomez, J., Cáceres, B., Ceballos, J. L., Basantes, R., Vuille, M., Sicart, J.-E., Huggel, C., et al.: Current state of glaciers in the tropical Andes: a multi-century perspective on glacier evolution and climate change, The Cryosphere, 7, 81–102, https://doi.org/10.5194/tc-7-81-2013, 2013.

Reynolds, R. L., Goldstein, H. L., Kokaly, R., Lowers, H., Breit, G. N., Moskowitz, B. M., Solheid, P., Derry, J., and Lawrence, C. R.: Light absorbing particles deposited to snow cover across the Upper Colorado River basin, Colorado, 2013–2016: Interannual variations from multiple natural and anthropogenic sources, Journal of Geophysical Research: Atmospheres, 130, e2024JD041 676, https://doi.org/10.1029/2024JD041676, 2025.

Saito, G., Asaoka, Y., Yamazaki, T., Mendoza, J., and Immerzeel, W. W.: Surface energy balance response to the 2014–2016 El Niño at Huayna-Potosí Glacier in the Tropical Andes, Hydrological Research Letters, 20, 82–89, https://doi.org/10.3178/hrl.25-00048, 2026.

https://doi.org/10.5194/egusphere-2026-5535
Preprint. Discussion started: 22 November 2026
© Author(s) 2026. CC BY 4.0 License.

Schmitt, C. G., All, J. D., Schwarz, J., Arnott, W. P., Cole, R., Lapham, E., and Celestian, A.: Measurements of light-absorbing particles on the glaciers in the Cordillera Blanca, Peru, The Cryosphere, 9, 331–340, https://doi.org/10.5194/tc-9-331-2015, 2015.

Schmitt, C. G., Schnaiter, M., Linke, C., and Arnott, W. P.: The light absorption heating method for measurement of light absorption by particles collected on filters, Atmosphere, 13, 824, https://doi.org/10.3390/atmos13050824, 2022.

Shi, T., Pu, W., Zhou, Y., Cui, J., Zhang, D., and Wang, X.: Albedo of black carbon-contaminated snow across northwestern China and the validation with model simulation, Journal of Geophysical Research: Atmospheres, 125, e2019JD032 065, https://doi.org/10.1029/2019JD032065, 2020.

Sicart, J. E., Hock, R., Ribstein, P., Litt, M., and Ramirez, E.: Analysis of seasonal variations in mass balance and meltwater discharge of the tropical Zongo Glacier by application of a distributed energy balance model, Journal of Geophysical Research: Atmospheres, 116, https://doi.org/10.1029/2010JD015105, 2011.

Sicart, J. E., Litt, M., Helgason, W., Tahar, V. B., and Chaperon, T.: A study of the atmospheric surface layer and roughness lengths on the high-altitude tropical Zongo glacier, Bolivia, Journal of Geophysical Research: Atmospheres, 119, 3793–3808, https://doi.org/10.1002/2013JD020615, 2014.

Skiles, S. M., Flanner, M., Cook, J. M., Dumont, M., and Painter, T. H.: Radiative forcing by light-absorbing particles in snow, Nature Climate Change, 8, 964–971, https://doi.org/10.1038/s41558-018-0296-5, 2018.

Soto Carrión, C., Schmitt, C. G., Zúñiga Negrón, J. J., Jiménez Mendoza, W., Arbieto Mamani, O., Pozo Enciso, R. S., Guevara Sarmiento, S. J., and Rado Cuchills, M. S.: Quantitative estimation of black carbon in the glacier Ampay-Apurimac, Journal of Sustainable Development of Energy, Water and Environment Systems, 9, 3–0, https://doi.org/10.13044/j.sdewes.d8.0342, 2021.

Torres, C., Suárez, L., Schmitt, C., Estevan, R., and Helmig, D.: Measurement of light absorbing particles in the snow of the Huaytapallana glacier in the central Andes of Peru and their effect on albedo and radiative forcing, Optica Pura y Aplicada, 51, 1–14, https://doi.org/10.7149/OPA.51.4.51004, 2018.

Villalobos-Puma, E., Morales, A., Martinez-Castro, D., Valdivia, J., Cardenas-Vigo, R., Lavado-Casimiro, W., and Santiago, A.: Dynamic atmospheric mechanisms associated with the diurnal cycle of hydrometeors and precipitation in the Andes–Amazon transition zone of central Peru during the summer season, Journal of Earth System Science, 133, 75, https://doi.org/10.1007/s12040-024-02278-3, 2024a.

Villalobos-Puma, E., Suarez, L., Gillardoni, S., Zubieta, R., Martinez-Castro, D., Miranda-Corzo, A., Bonasoni, P., and Silva, Y.: Atmospheric black carbon observations and its valley-mountain dynamics: eastern cordillera of the central Andes of Peru, Environmental Pollution, 355, 124 089, https://doi.org/10.1016/j.envpol.2024.124089, 2024b.

Warren, S. G.: Optical properties of ice and snow, Philosophical Transactions of the Royal Society A: Mathematical, Physical and Engineering Sciences, 377, https://doi.org/10.1098/rsta.2018.0161, 2019.

Weber, A. M., Beaudon, E., Sierra-Hernández, M. R., Davis, M., Kenny, D., Shutkin, T. Y., and Thompson, L. G.: On the influence of mineral dust on glacial albedo at Nevado Huascarán (Cordillera Blanca, Peru), Journal of Geophysical Research: Atmospheres, 131, e2025JD045 574, https://doi.org/10.1029/2025JD045574, 2026.

Whicker, C. A., Flanner, M. G., Dang, C., Zender, C. S., Cook, J. M., and Gardner, A. S.: SNICAR-ADv4: a physically based radiative transfer model to represent the spectral albedo of glacier ice, The Cryosphere, 16, 1197–1220, https://doi.org/10.5194/tc-16-1197-2022, 2022.